Advancements in Understanding the 2-D Role of Impurity Radiation for Dissipative Divertor Operation on DIII-D

by

C.M. Samuell (LLNL)

A.G. McLean, S.L. Allen, M.E. Fenstermacher, C.J. Lasnier, W. Meyer, G.D. Porter, T. Rognlien, F. Scotti, V. Soukhanovskii (LLNL), A. Holm, A.E. Jaervinen, M. Groth (Aalto University), C. Johnson (Auburn), J. Boedo, E.M. Hollmann (UCSD), F. Glass, H. Guo, A.W. Leonard, A.L. Moser, D. Thomas, H.Q. Wang (GA), J.D. Watkins (SNL), and the DIII-D Team

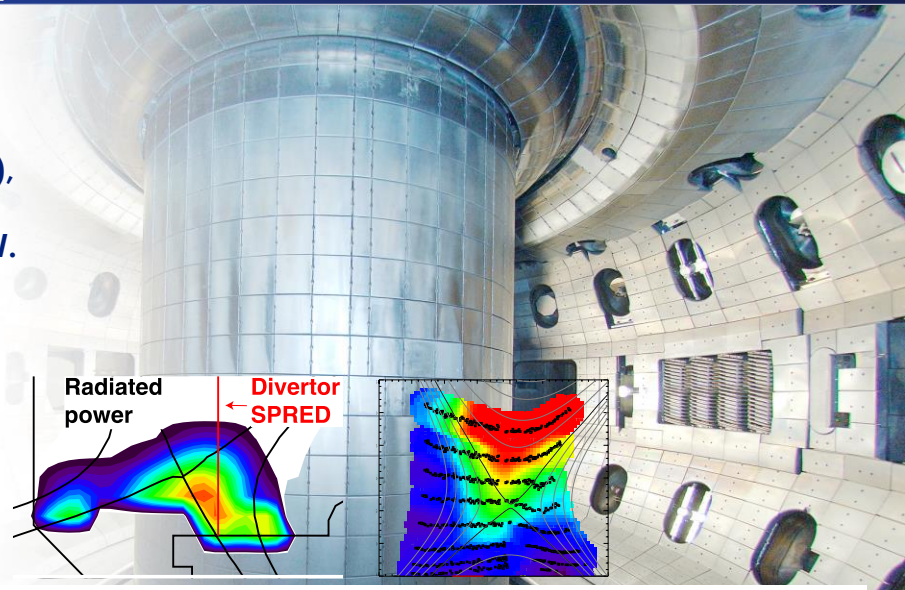

Presented at the

The 28th International Atomic Energy Agency Fusion Energy Conference (FEC 2020)

May 10-15, 2021

P1 Posters 1 - Virtual
Tuesday 08:30 AM

https://conferences.iaea.org/event/214/contributions/17149/

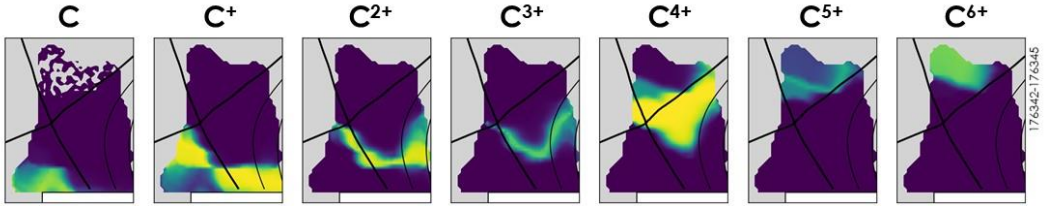

Prepared by LLNL under DE-FC02-04ER54698, DE-AC52-07NA27344, and LLNL LDRD project 17-ERD-020. This report was prepared as an account of work sponsored by an agency of the United States Government. Neither the United States Government nor any agency thereof, nor any of their employees, makes any warranty, express of implied, or assumes any legal liability of responsibility for the accuracy, completeness, or usefulness of any information, apparatus, product, or process disclosed, or represents that its use would not infringe privately owned rights. Reference herein to any specific commercial product, process, or service by trade name, trademark, manufacturer, or otherwise does not necessarily constitute or imply its endorsement , recommendation, or favoring by the United States Government or any agency thereof, The views and opinions of authors expressed herein do not necessarily state or reflect those of the United States Government or any agency therefor.

Outline

1. **Leveraging the broad array of measurements on the DIII-D tokamak has been used to elucidate the physics underlying 2-D detachment processes in the divertor**

2. **Combination of EUV/VUV-VIS-IR spectroscopy, ColRadPy collisional radiative modeling, and 2-D T_e and n_e measurements from Divertor Thompson Scattering have been used to infer divertor impurity densities**
   - Inferred spatial profiles reveal a greater radial emission extent compared to UEDGE fluid modeling with full ExB drifts

3. **Analysis reveal the 2-D nature of detachment is critically important for design of detachment scenarios for next stage devices**

Motivation: Predictions of impurity concentration required for detachment in future machines need experimental validation

- **Typical plasma will radiate 40-90% of input power**
  - More radiation necessary to 'detach' the divertor
- ***Critical to know impurity content necessary for detachment***
  - Radiation from deuterium alone is not enough
- **Scalings have major implications for future machines**
  - **Upstream conditions**: R.J. Goldston, *et. al.*, PPCF 59 (2017) 055015
  - **Machine size scaling**: M.L. Reinke, *et al.*, NF 57 (2017) 034004
  - **Energy/mom. loss scaling**: A. Kallenbach, *et al.*, PPCF 58 (2016) 045013
  - ***Projection of ~10% impurity fraction required in ITER, ~20% for DEMO***
    - Fuel dilution, poor fusion performance
  - However, these rely on 1D scalings
    - ***Need experimental validation on current machines***

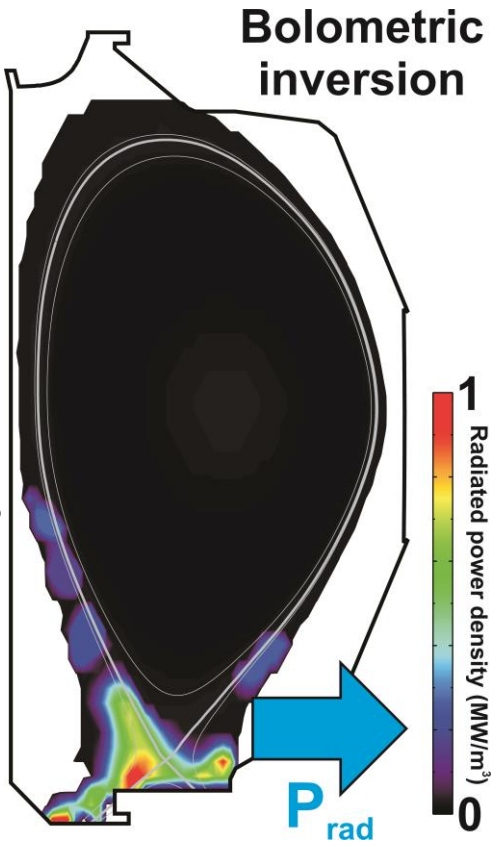

Recent work (past ~10 years) to characterize divertor impurity concentrations demonstrates the challenges involved

- **JT-60: VUV and visible C emissions**
  - T. Nakano, et al., NF 47 (2007) 1458
  - T. Nakano, *et al.*, JNM 390-391 (2009) 255

- **JET/ASDEX-U: Visible N II emissions**
  - S. Henderson, et al., NF 58 (2018) 016047
  - S. Henderson, *et al*., NME 18 (2019) 147

- ***Both approaches rely on local plasma parameters inferred from spectroscopic line ratios***
  - ***Current work uses unique combination of local T_e,n_e and absolutely calibrated VUV emissions***

- **Carbon wall + erosion presents the same physics as metal wall + extrinsic impurity**

Nakano, JT60

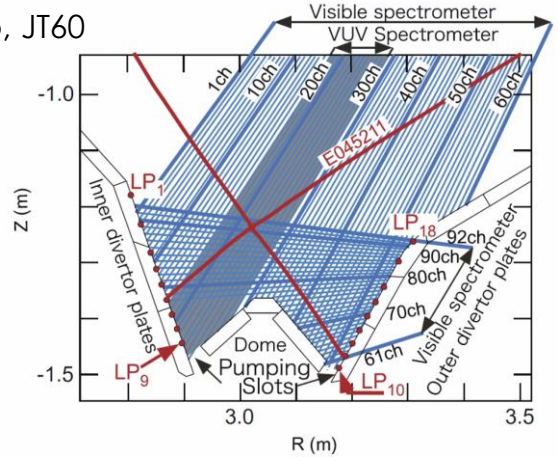

Henderson
IAEA Div. Conc. 2019

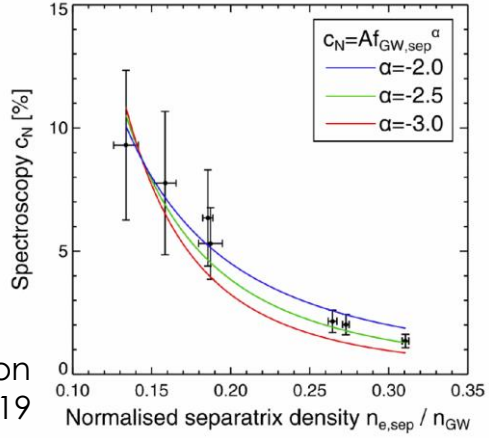

Our approach for determining concentrations relies on an iterative comparison between measured and synthetic spectra

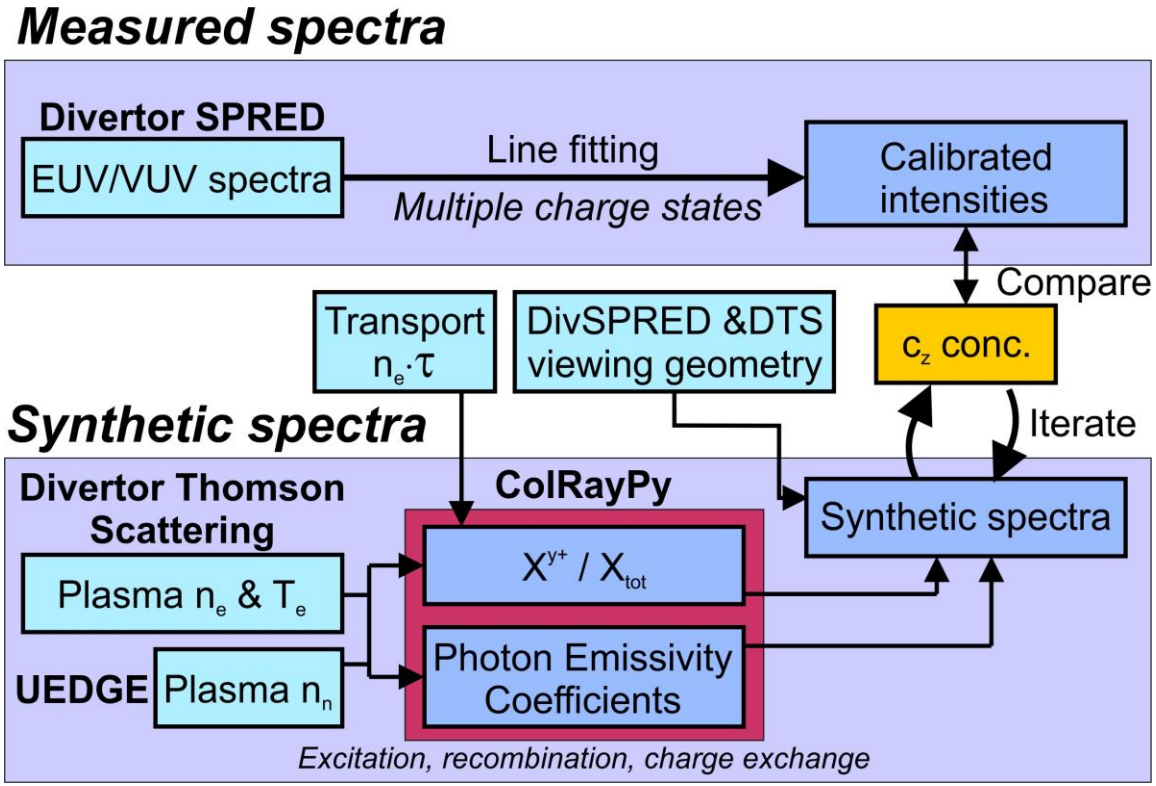

DIII-D NATIONAL FUSION FACILITY

Measuring impurity concentrations relies on quantitative accounting of impurity emissions in known plasma conditions

- **Observed emission is a product of atomic processes occurring for all plasma species**
  - Excitation/deexcitation, ionization, recombination
  - Rates determined by local plasma conditions
- **For known conditions along a line of sight:**
  - Measured spectrum can be taken
  - The charge state distribution for each species may be calculated
  - A synthetic spectra can be created
  - Brightness of measured vs. synthetic spectra determines the conc.

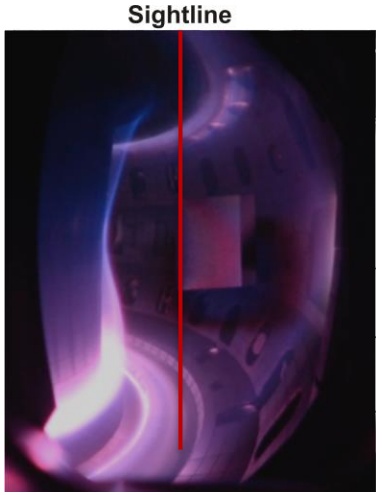

Spectrum-spanning calibrated radiance in DIII-D plasma

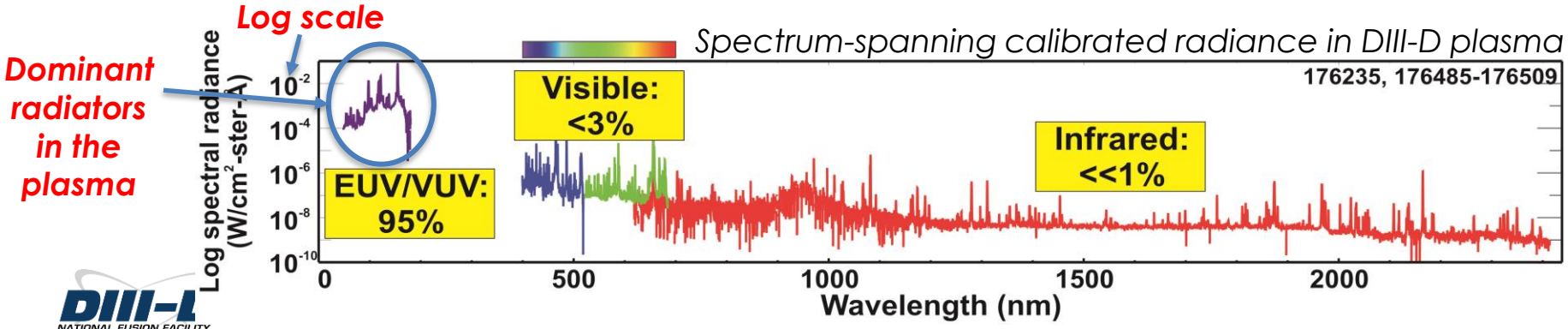

DIII-D NATIONAL FUSION FACILITY

Resonance spectral emissions offer the distinct advantage of direct interpretability

- **Volume emission rate, coronal excitation and emission, optically thin:**
  - $E_{ij} = Br_{ij}\, Q_{gnd \rightarrow p}\, n_i\, n_e$ J.L. Terry, *et al*., NF 18 (1978) 485
    - Br: branching ratio to lower level, Q: electron impact excitation rate [T_e, n_e]
- **For resonance emission (Br=1), brightness along line-integrated sight:**
  - $B = 1/(2\pi) \int (Q\, n_i(z)\, n_e(z)\, dz)$
- **Valid for ions with no metastable levels: Li-like ion lines O VI, N V, C IV**
  - With metastables, level populated by ionization from next lower charge state, plus excitation from ground
- **For low and medium-Z elements, resonance emissions are primarily in the EUV/VUV spectral region**
  - *Calibrated EUV/VUV spectra is a challenge compared to UV/VIS/NIR*
  - **Available with divertor view on DIII-D: 'DivSPRED'**
    - SPRED: Survey, Poor Resolution, Extended Domain (45-170 nm)
    - Originally calibrated at NIST SURF
    - Adapted using branching ratio technique
  - **Similar capability on JET, TCV, and MAST-U**

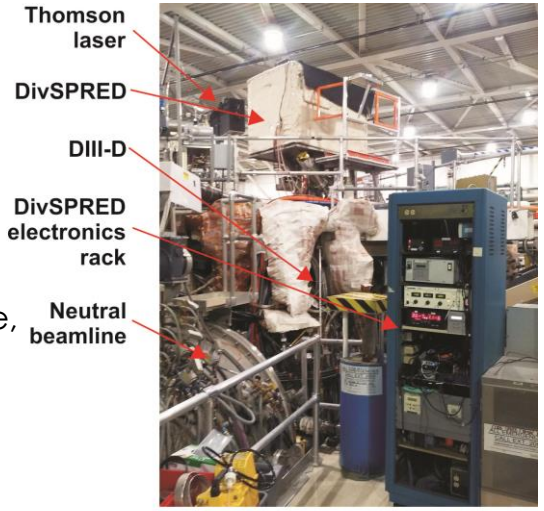

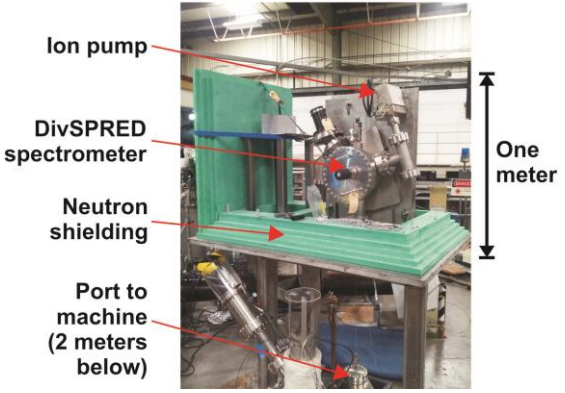

DIII-D NATIONAL FUSION FACILITY

Seven distinct emission lines chosen for carbon workflow: C^{1+}, C^{2+} & C^{3+}

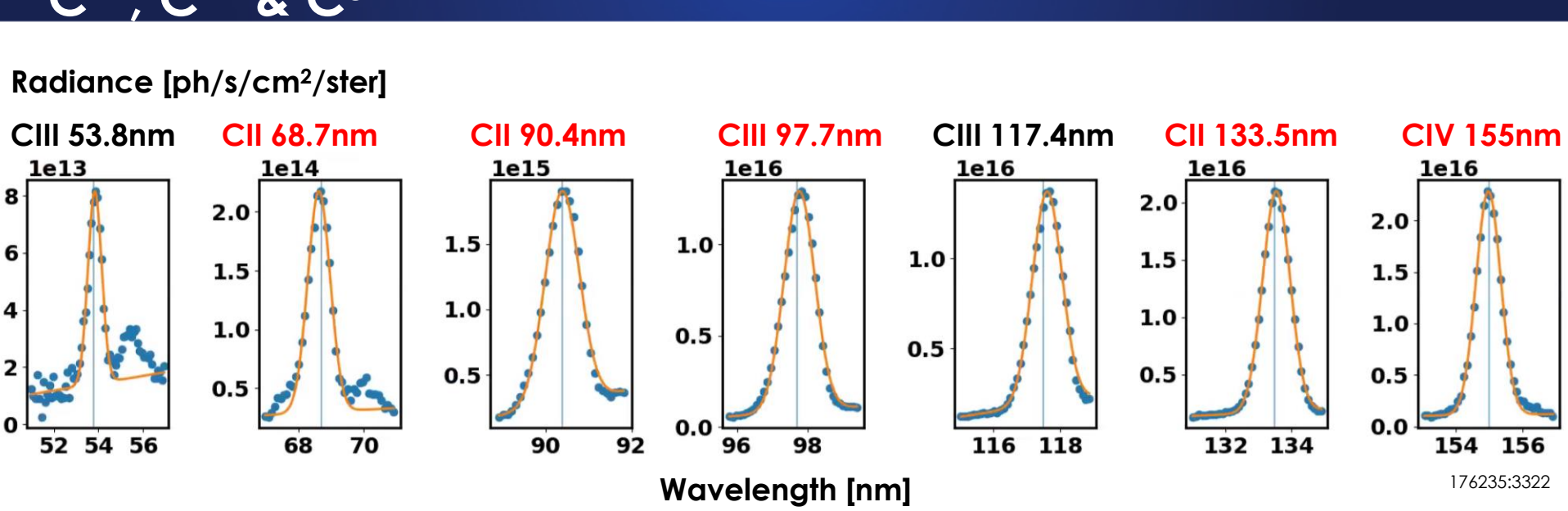

Resonance lines in red

- **Each line is separately fit with a ~1nm FWHM gaussian characteristic of the instrumental width, linear background subtraction**
- ***Similar capability for nitrogen: N II, N III, N IV, and N V emissions in the observed bandwidth for DivSPRED***

DIII-D NATIONAL FUSION FACILITY

Divertor Thomson scattering (DTS) provides T_e and n_e critical to interpretation of line-integrated spectra

- T_e, n_e coincident with emitting volume measured by DivSPRED
- 8 ch system until 2019
- *12 ch system for 2020*
- OSP sweeping
  - Data mapping/reconstruction

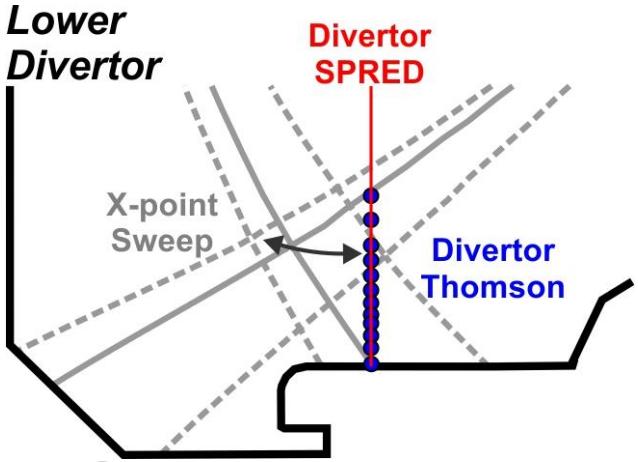

1D profile from single time-slice

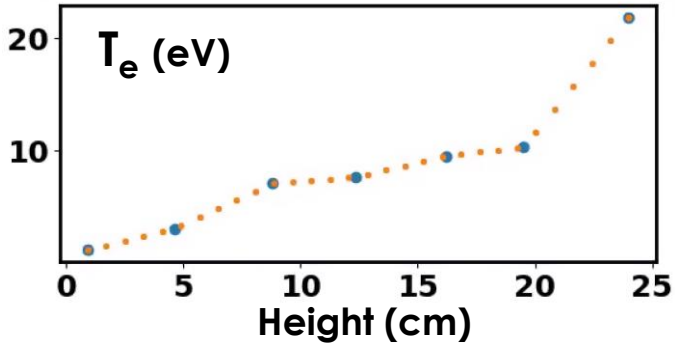

2D profile from many time-slices

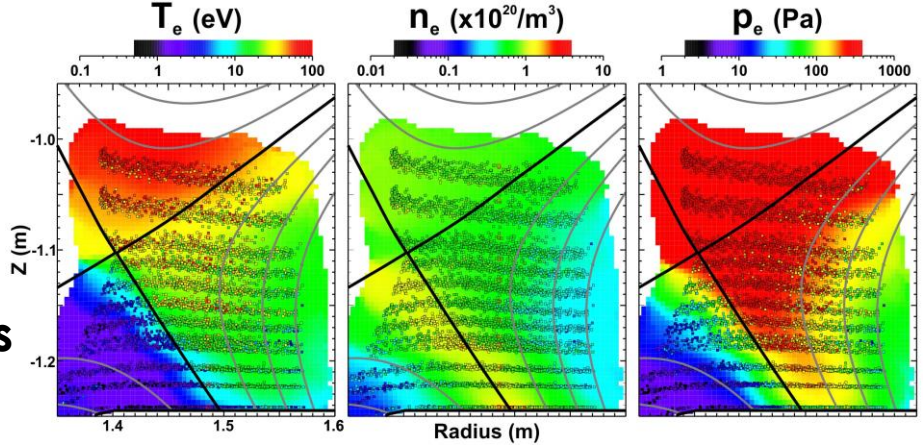

DIII-D NATIONAL FUSION FACILITY

Model for synthetic spectra incorporates variables for CX by neutrals, and $n_e \cdot \tau$ for transport

- **Neutrals**

$$\epsilon_{i \to j_{CX}} = \sum_{\rho} \mathrm{PEC}^{CX}_{\rho, i \to j} n_H n_\sigma^{(z+1)+}$$

- **Transport**
  - $n_e \cdot \tau$: 'Non-coronal enhancement factor'
  - Residence time τ; <1 ms for low T_e, upper limit of inverse ELM frequency

- ***Adding CX, and lowering $n_e \cdot \tau$ allow charge states to exist at higher local T_e***

- ***Analysis framework allows for easy adjustment of these factors***
  - *Better match diagnostic data and test models*

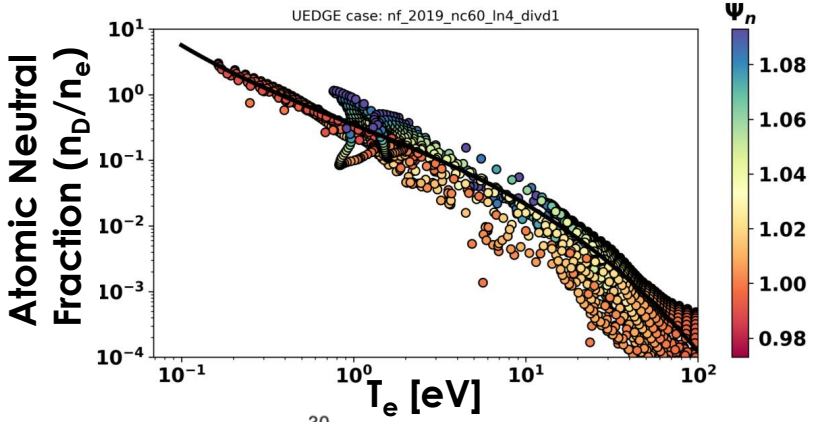

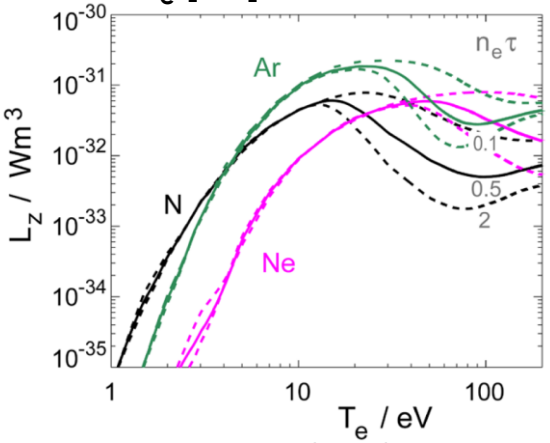

A. Kallenback, *et al.*, PPCF 58 (2016) 045013
L. Casali, *et al.*, CPP 58 (2018) 725

ColRadPy provides a collisional radiative solution for given plasma conditions

- **Collisional radiative model built in python**
  - Spans Coronal (low density) and LTE (high density) cases
  - Johnson, Lock, Ennis, NME 20 (2019) 100579

Curt Johnson, *et al.*, FO34(B) Friday "Collisional Radiative Modeling of Tungsten for Gross and Net Erosion"

- **Inputs:**
  - Electron density and temperature (DTS)
  - Atomic physics (i.e., ADAS adf04 files)

- **Outputs:**
  - Ionization and recombination rates
  - Balance of charge states
  - Photon Emissivity Coefficient (PEC) values
    - Compared to data in ADAS adf15 PEC files
  - ***Brightness of any given line or set of set lines***
    - Distribution dependent on divertor conditions

C. Samuell, *et al.*, RSI (submitted) 2020

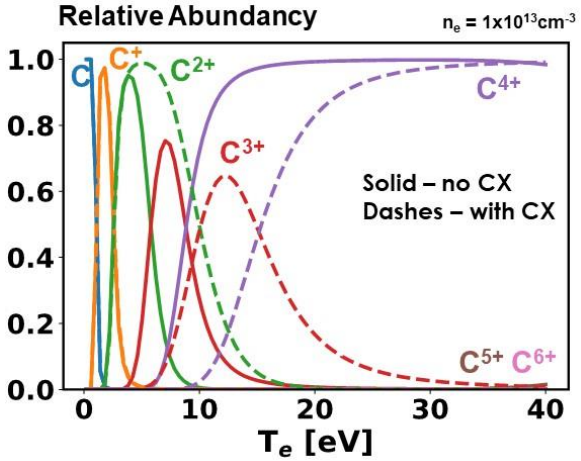

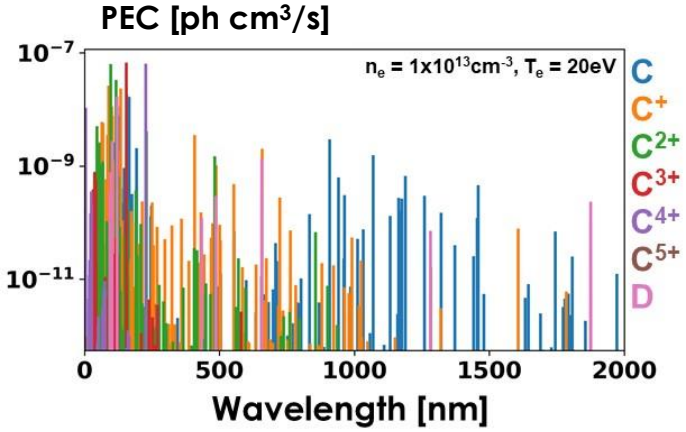

DIII-D NATIONAL FUSION FACILITY

Synthetic spectra is the summation of emission contributions for conditions along the line of sight

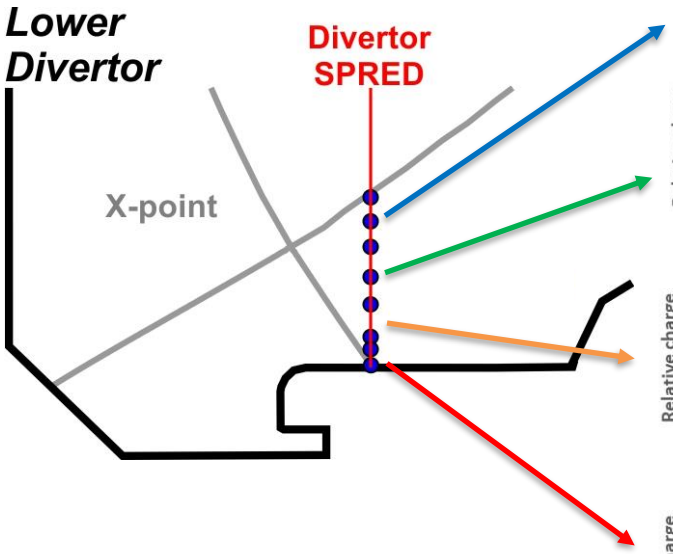

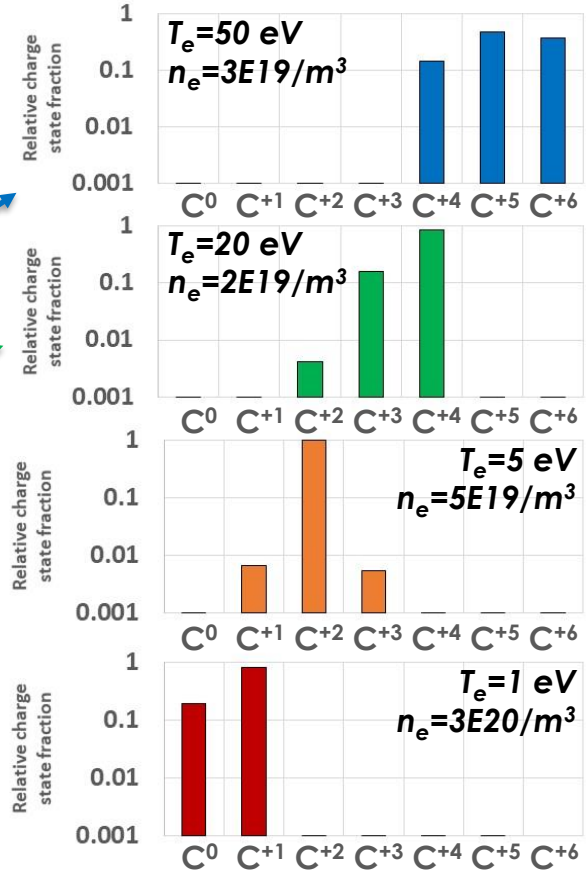

Contributions summed along line-of-sight for iterated n_C/n_e

176235, 4040 ms: C fraction=0.2%

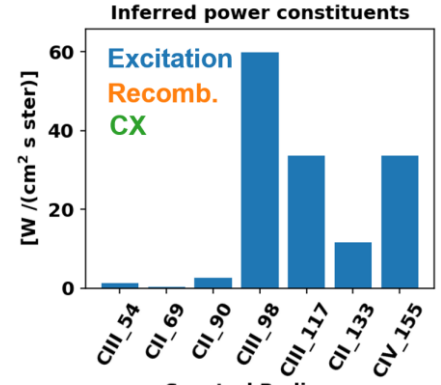

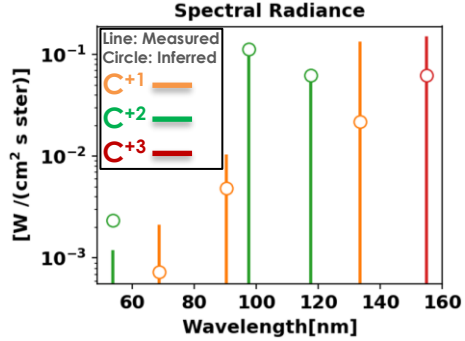

DIII-D NATIONAL FUSION FACILITY

Evolution of impurity fraction appears gradual despite sharp detachment drop

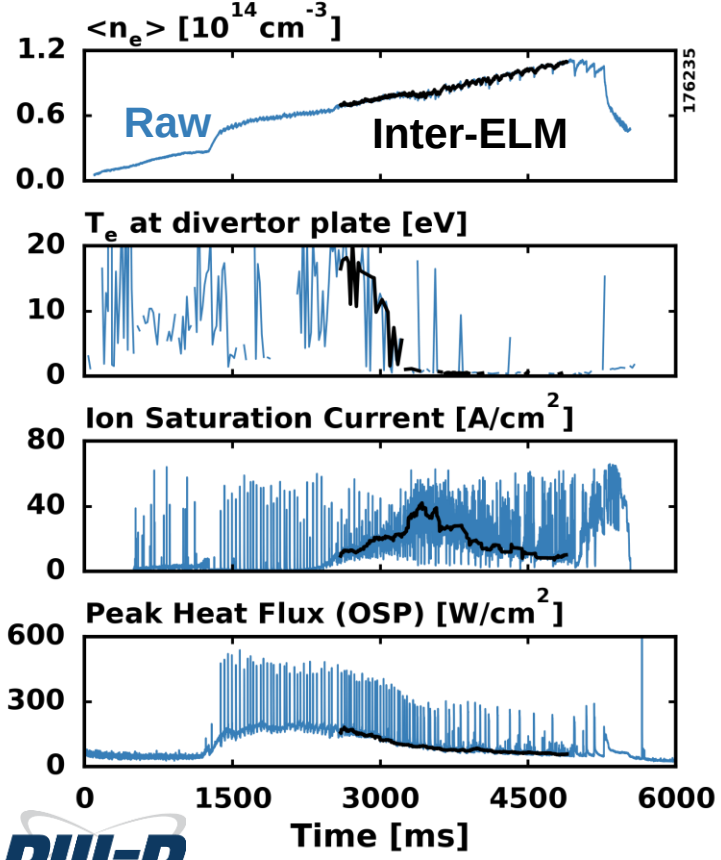

- Example of a density ramp with fixed strike point
  - Attached (~20 eV) plasma transition to detached (<1 eV)

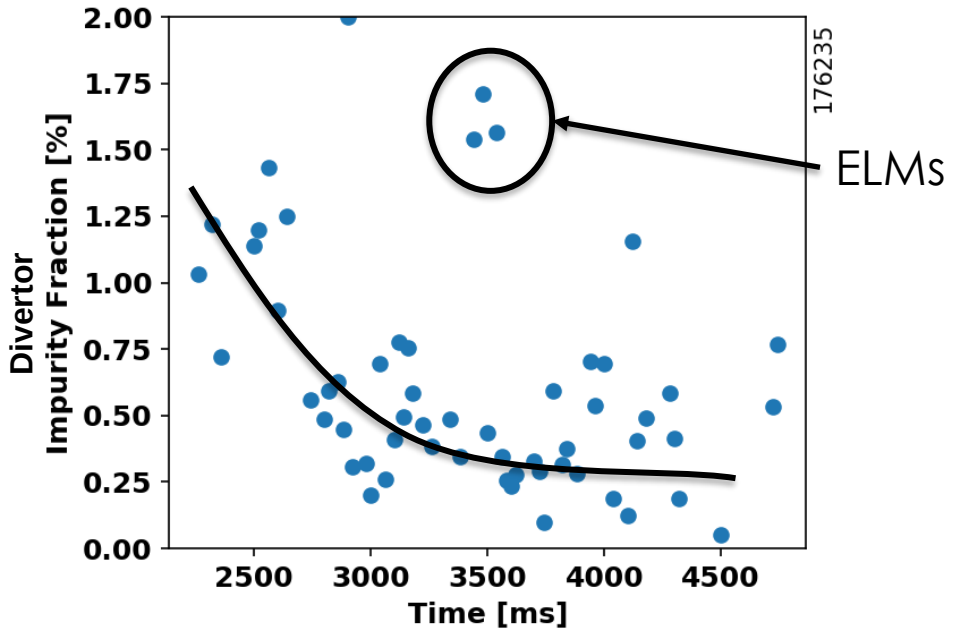

Significant departure from a fixed divertor impurity fraction assumption for modeling

DIII-D NATIONAL FUSION FACILITY

Divertor impurity fraction falls with upstream density, Close agreement with Goldston model for detachment threshold

- Divertor impurity fraction
- Inter-ELM only
  - Filtered to 30-95% of ELM cycle
- Demonstrates similar loss in magnitude in transition to detachment

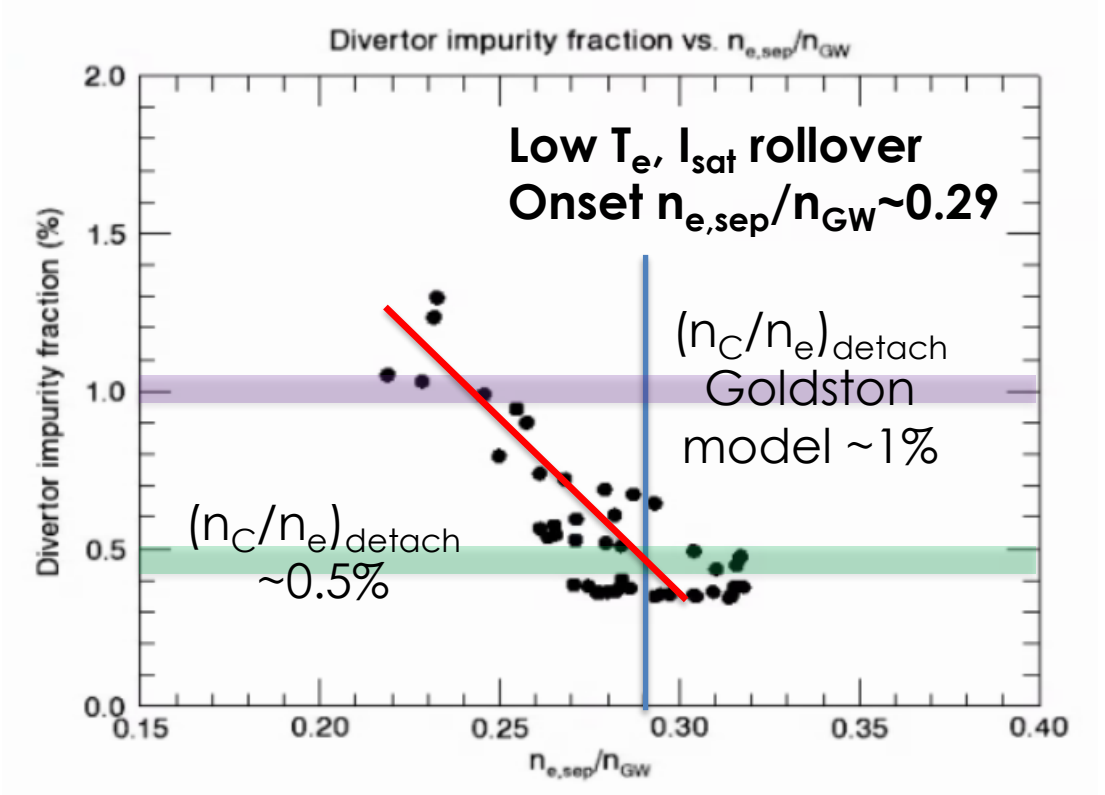

DIII-D NATIONAL FUSION FACILITY

Comparing attached and detached divertors shows differences in the dominant impurity species near the target surface

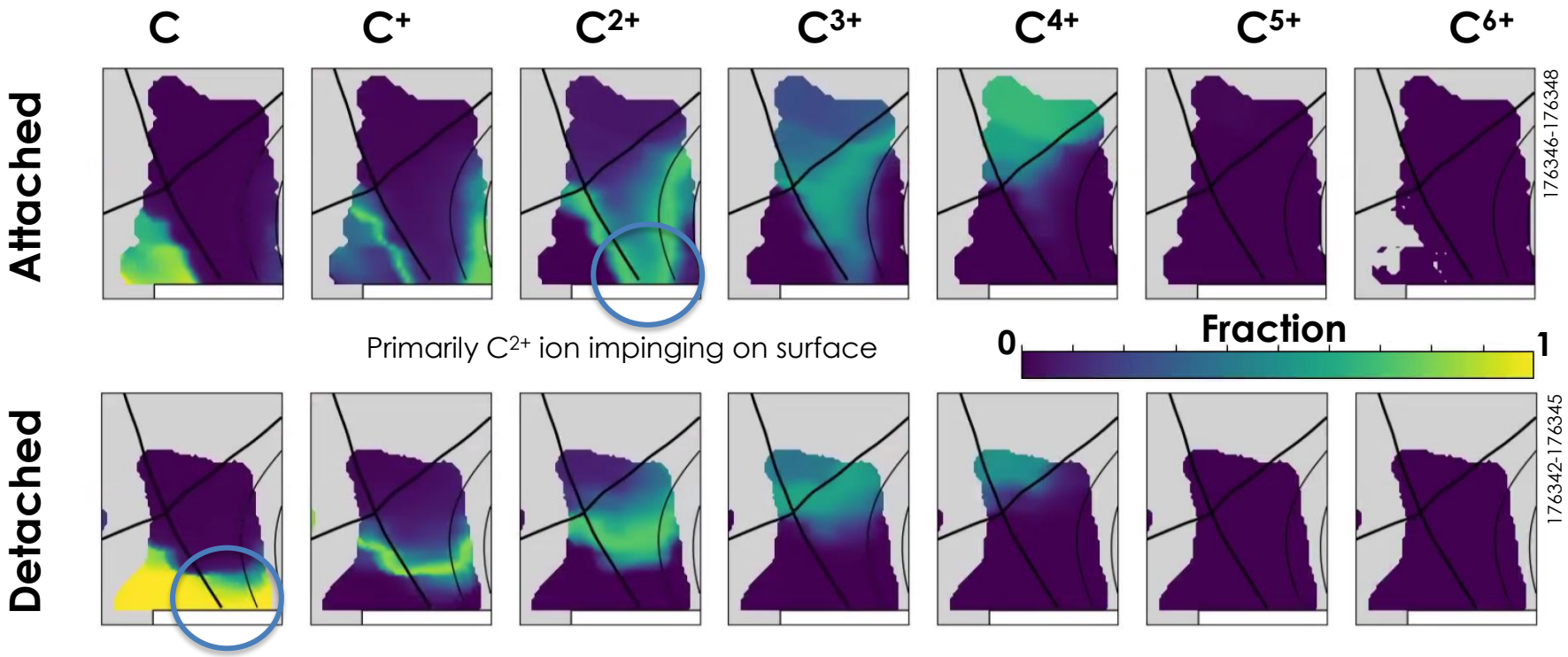

Case with n_e*tau = 2E9 cm^{-3} s

ColRadPy model allows ease of investigation of neutral role and transport

DIII-D NATIONAL FUSION FACILITY

UEDGE comparison for the detached case suggests transport playing a smaller role that determined by the code

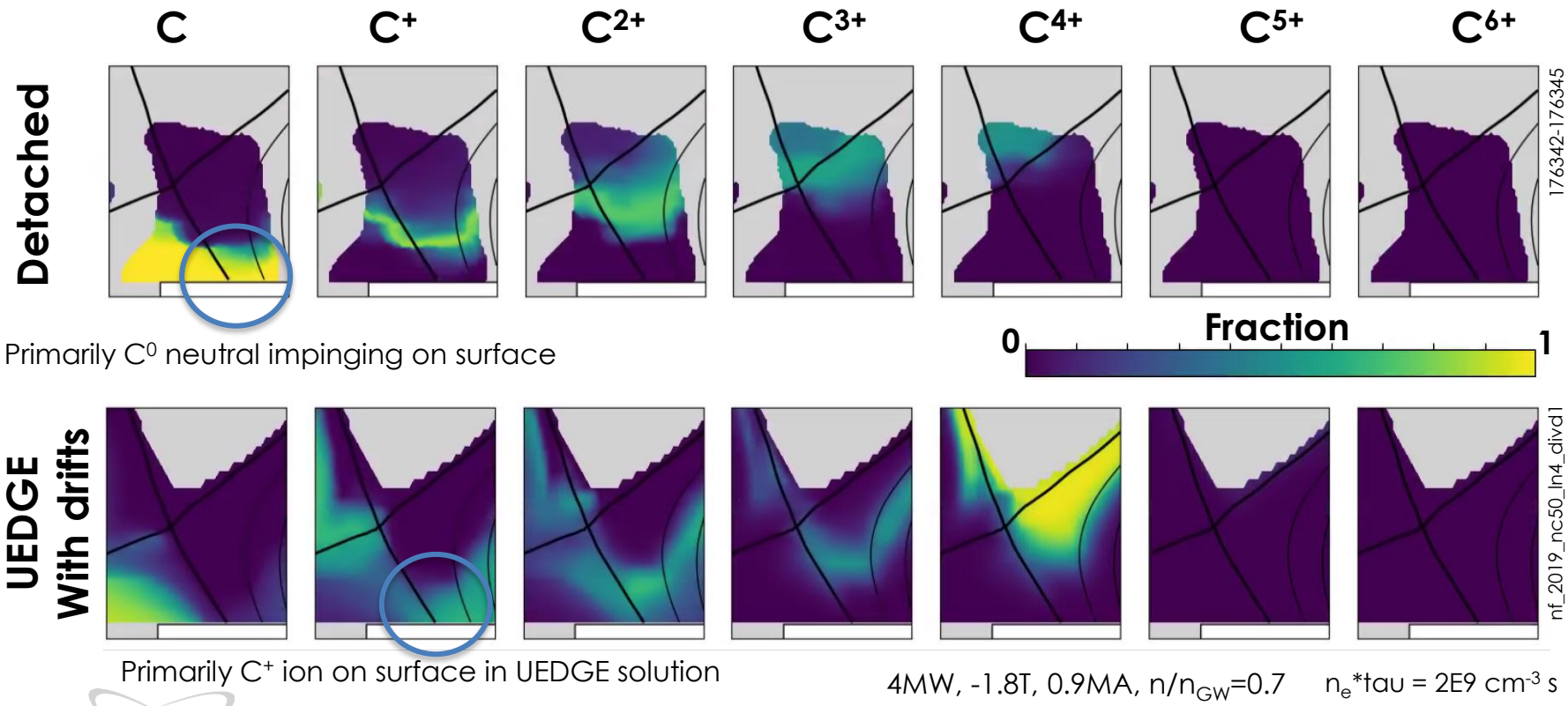

4MW, -1.8T, 0.9MA, n/n_{GW}=0.7 n_e*tau = 2E9 cm^{-3} s

Powerful tool for quantitative code validation spanning divertor conditions

UEDGE comparison for the detached case suggests transport playing a smaller role that determined by the code

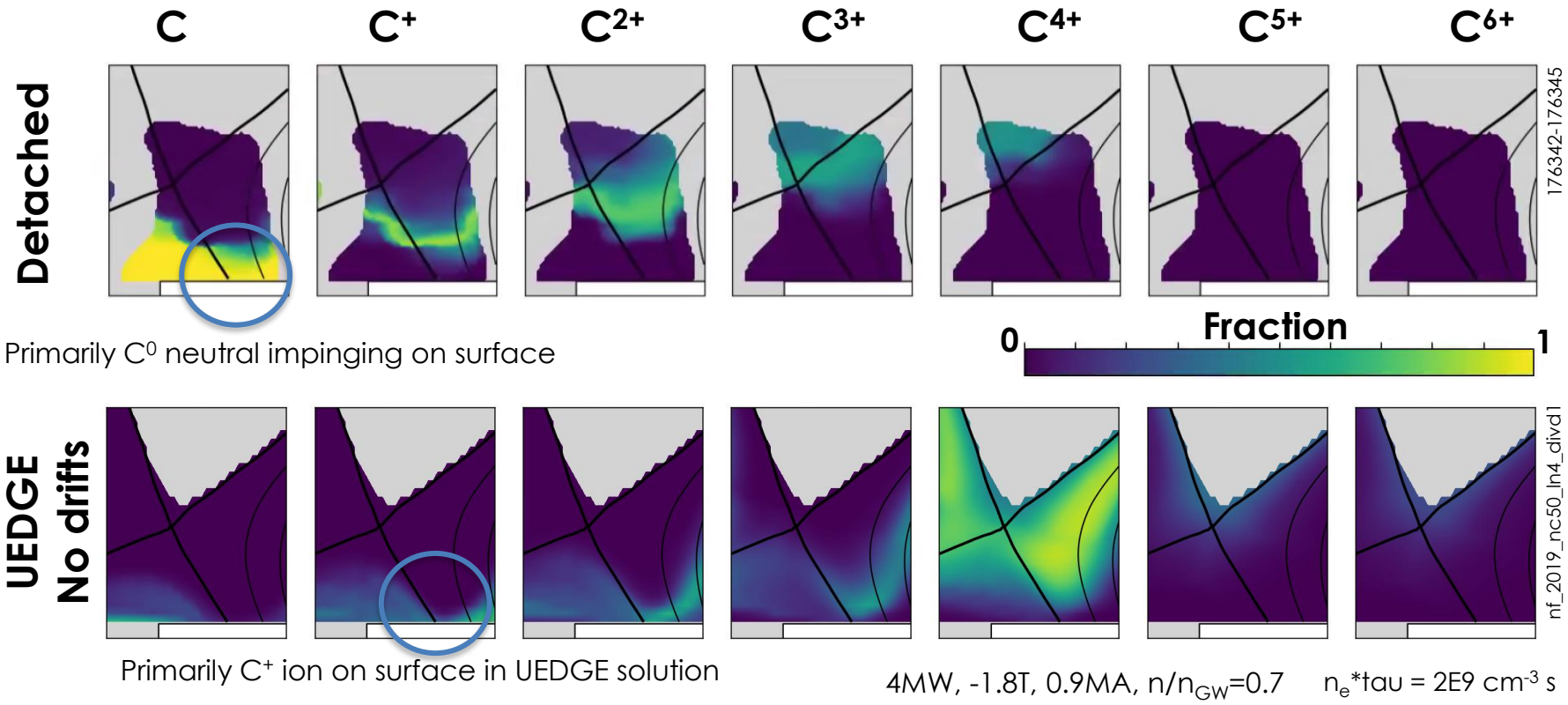

Powerful tool for quantitative code validation spanning divertor conditions

The radial extent of the radiative volume in detached H-mode discharges is much broader compared to UEDGE fluid modeling

- **Increasing level of broadening observed at higher powers**
- **Observed in both charge-state resolved line emission and total radiated power (bolometry), DTS, and 2-D imaging**
- **Poloidal E × B drift can dominate the poloidal heat transport in the radiative front**
- **Larger extent provides opportunity for greater dissipation volume**
  - Demonstrates that fully-2D simulations including cross-field drifts are required for detachment studies
  - Working towards a predictive capability of divertor heat loads

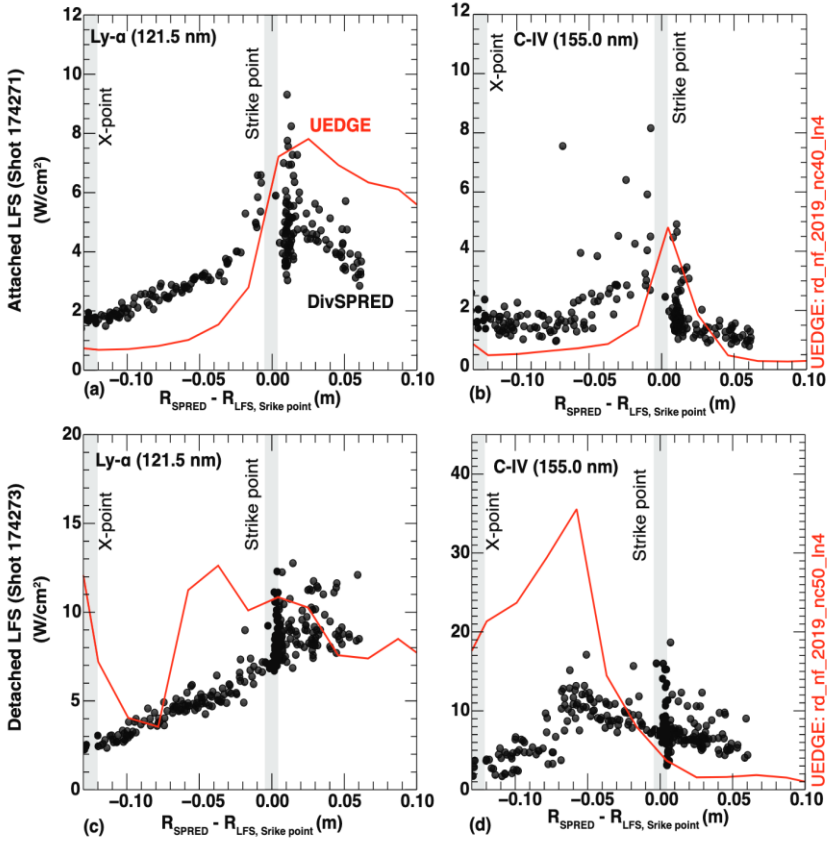

DIII-D NATIONAL FUSION FACILITY

Conclusions: Ensemble of divertor diagnostics on DIII-D allows for impurity concentration measurements in all plasma conditions

- **Inter-ELM intrinsic carbon impurity fraction in DIII-D is measured, showing**
  - *n_C/n_e at detachment onset consistent with model prediction for evaluated cases*
  - *Significant departure from a fixed divertor impurity fraction assumption for modeling*
- **Absolutely calibrated spectroscopy and local divertor Thomson scattering**
  - Provide a unique and powerful combination of divertor diagnosis capabilities
- **Flexible framework and workflow to evaluate the impact of divertor processes**
  - ColRadPy collisional radiative model incorporates all relevant atomic physics and allows reconstruction of the charge state distribution and emission profile
- **Future experiments on DIII-D provide critical benchmarks for code validation and detachment scalings**
  - Insight into divertor/scrape-off-layer (SOL) impurity transport using 2D visible imaging
  - Reveal how efficiently the intrinsic impurity can be complemented with extrinsic sources

Backup slides

Future device studies with UEDGE have shown lower impurity concentrations at detachment than scalings predict

- **Rognlien, Rensink, Stotler, FED 135 (2018) 380**
  - FNSF modeling with UEDGE and DEGAS 2
  - 0.15-0.4% fixed Neon fraction
  - Weakly detached inner leg, strongly detached outer leg (T_e~1eV)
- **Rensink and Rognlien, FST 67 (2014) 125**
  - ARIES-ACT modeling with UEDGE
  - Cases with 0.4% fixed Ne, or 0.04% fixed Ar
- **Within ~factor of 2 for full multi-charge state cases**

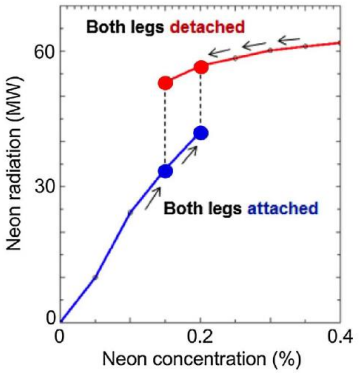

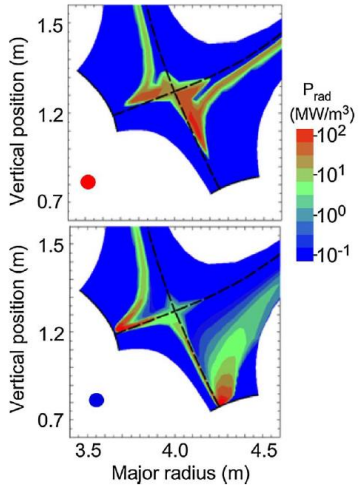

Huber, Chankin, NF (2021) accepted

	Nitrogen			Neon			Argon		
	L_{INT} (10^{-36} W m^3 eV$^{1/2}$)	$c_{Z=7}$ (%) in D plasmas	$c_{Z=7}$ (%) in D-T plasmas	L_{INT} (10^{-36} W m^3 eV$^{1/2}$)	$c_{Z=10}$ (%) in D plasmas	$c_{Z=10}$ (%) in D-T plasmas	L_{INT} (10^{-36} W m^3 eV$^{1/2}$)	$c_{Z=18}$ (%) in D plasmas	$c_{Z=18}$ (%) in D-T plasmas
ASDEX-U	5.7	1.6	1.2*	24.2	0.38	0.28*	44.8	0.18	0.13*
JET-ILW	6.6	3.4	2.5	27.6	0.83	0.61	52.9	0.38	0.28
ITER	14.9	14.7	10.8	44.5	4.9	3.6	131.8	1.48	1.1
EU DEMO 1	18.8	24.3	17.9	50.6	9.0	6.6	163.6	2.5	1.8

Table 2. Estimated impurity fractions required for detachment for N_2, Ne and Ar assuming f_{LH}=1.2, f_{ne}=0.9 and $n_e\tau = 1.0 \times 10^{20}$ m^{-3} ms. Calculation are made for pure D and mixed D-T (50%D/50%T) plasmas.

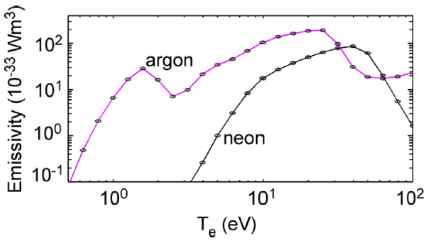

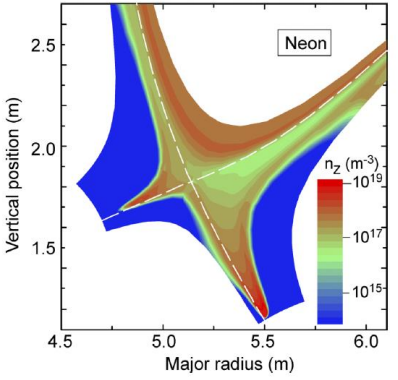

DIII-D NATIONAL FUSION FACILITY

DivSPRED on DIII-D is capable of quantifying emissions from a variety of impurities

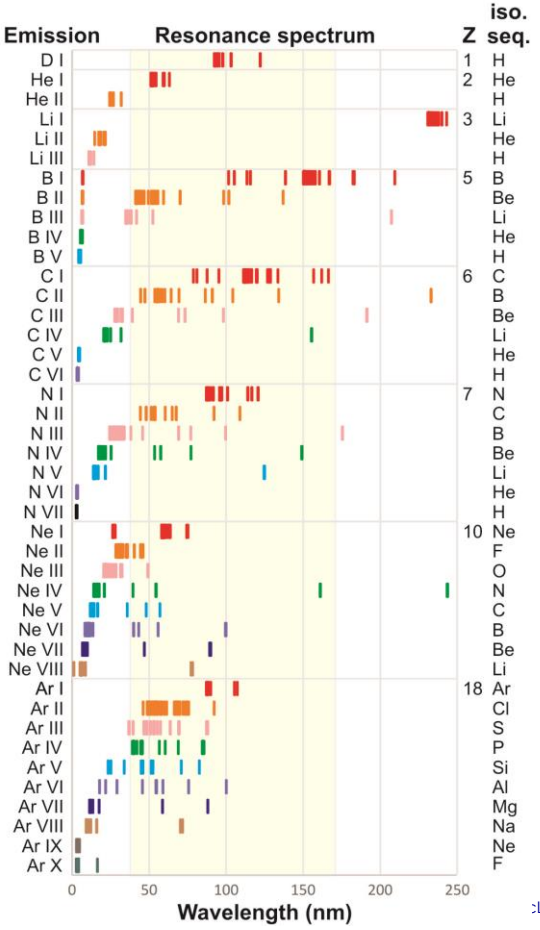

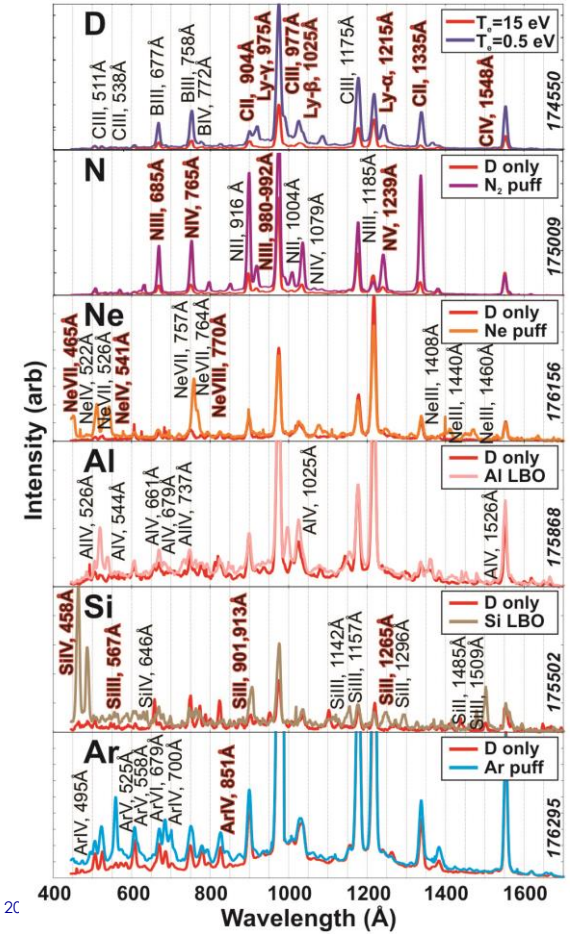

DIII-D NATIONAL FUSION FACILITY

Goldston model for impurity concentration at detachment predicts ~1% N (or C) in DIII-D with P_{sep}=2.5 MW

	C-Mod	DIII-D	ASDEX-U	JET	ITER	FNSF (A=4)	EU Demo 1
P_{sep} (MW)	3.83	2.5	10.7	14	100	96	154.7
B_T (T)	5.4	2	2.5	2.5	5.3	7	5.7
R_0 (m)	0.7	1.73	1.6	2.9	6.2	4.5	9.1
P_{sep}/R	5.47	1.45	6.69	4.83	16.13	21.33	17.00
$P_{sep}B_T/R$	29.55	2.89	16.72	12.07	85.48	149.33	96.90
I_p (MA)	0.82	1.3	1.2	2.5	15	7.5	20
A (m)	0.22	0.59	0.52	0.9	2	1.13	2.94
κ_{95}	1.51	1.64	1.63	1.73	1.8	2.1	1.7
$\langle B_p \rangle$ (T)	0.58	0.33	0.34	0.39	1.03	0.81	0.98
q_{cyl}	3.75	2.81	3.23	2.81	2.42	3.57	2.62
n_{GW}	5.39E+20	1.19E+20	1.41E+20	9.82E+19	1.19E+20	1.87E+20	7.37E+19
Proj. c_N	1.0%	1.0%	4.0%	4.0%	10.0%	8.5%	18.5%

Large values suggest a challenge for pedestal and core compatibility

DIII-D NATIONAL FUSION FACILITY

Impurity fraction is a critical component for detachment control & physics understanding

- **Understanding & predicting detachment.**
  - Metal walled devices require impurity-driven detachment
  - Impurities play a dominant role for detachment in DIII-D even in "unseeded" discharges
    - Are carbon and nitrogen equivalent?
  - What level of impurity seeding is required for a fusion reactor to detach?

$$c_z \propto \frac{P_{\mathrm{sep}}}{\langle B_p \rangle (1+\kappa^2)^{3/2} (n_{\mathrm{sep}}/n_{\mathrm{GW}})^2 l_{||}^*} \quad (1)$$

$$c_z \approx B_T^{0.88} R^{1.33} \quad (2)$$

$$c_z \approx \frac{P_{\mathrm{sep}}/R}{p_0 \lambda_{\mathrm{int}} R^{r_z}} \quad (3)$$

Scalings are 1D or 0D!

(1) Goldston R 2017 PPCF 59 055015
(2) M.L. Reinke 2017 Nucl. Fusion 57 03400
(3) A Kallenbach et al 2016 PPCF 58 045013
Henderson, IAEA Div Con, 2019

Carbon Impurity fraction in detached plasmas inferred to be around 0.1-0.5%

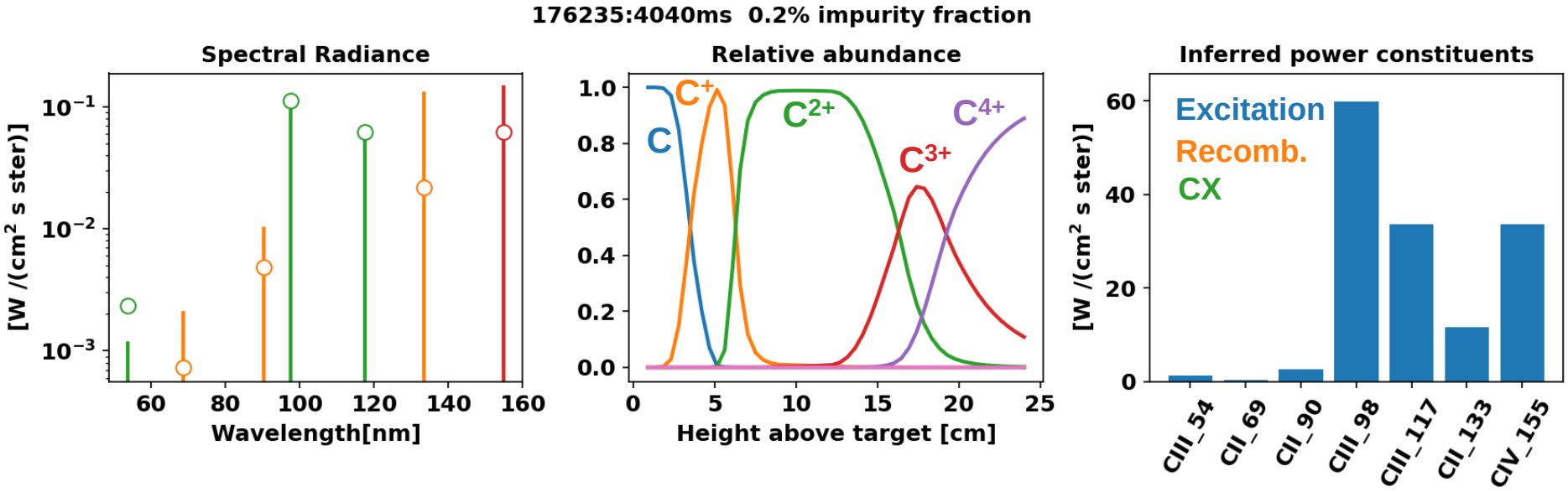

Lines = measured
Circles = inferred

- **Recombination and CX plays a role in the ionization balance; but not total emissivity**

DIII-D NATIONAL FUSION FACILITY

Transport, n_e*tau, value used affects the charge state balance

ne*tau [m^{-3} ms]

2E20

0.2E20

0.02E20

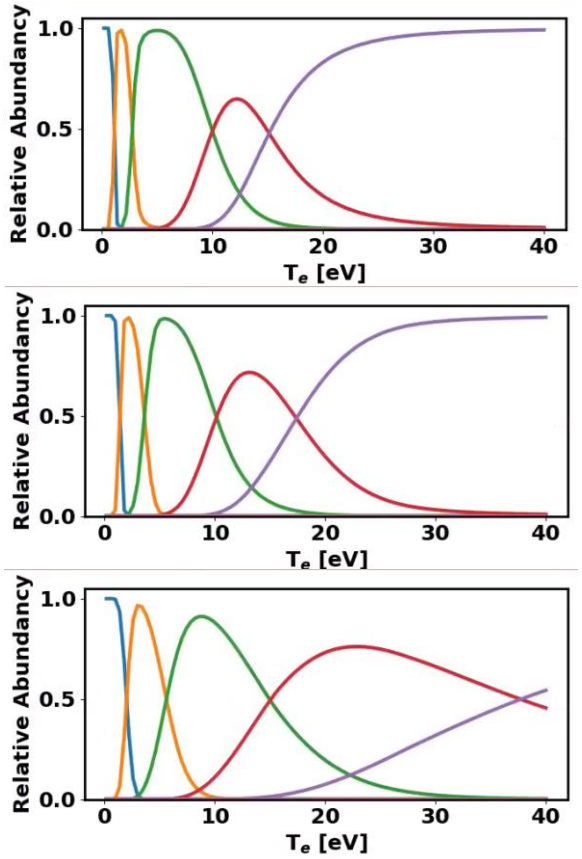

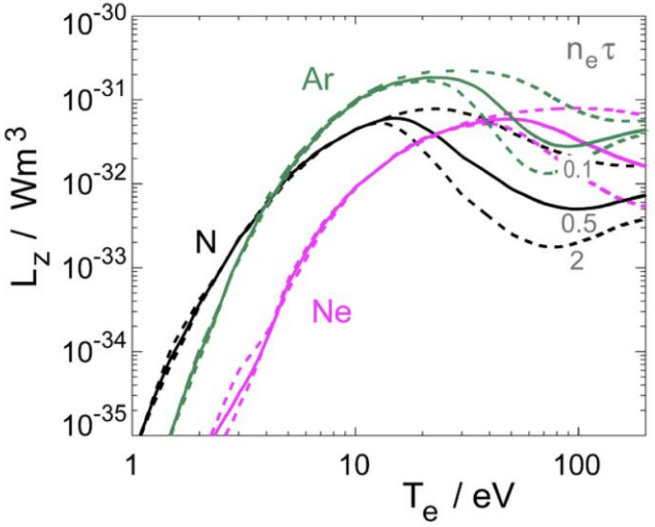

Figure 3. Radiative loss functions calculated from ADAS for possible divertor seeding gases N, Ne, Ar and $n_e = 1 \cdot 10^{20}$ m^{-3}. Solid lines have been calculated for the non-coronal parameter $n_e\tau = 0.5$ as used throughout this study, the upper and lower dashed lines for each species correspond to values $n_e\tau = 0.2$ and $2 \cdot 10^{20}$ ms m^{-3}.

Kallenbach 2016 PPCF

Resonance spectral emissions offer the distinct advantage of direct interpretability

- **Volume emission rate: $E_{ij} = B_{ij}\, Q_{gnd \rightarrow p}\, n_i\, n_e$**
  - E: emission rate, B: branching ratio to lower level, Q: electron impact excitation rate
- **Valid for ions with no metastable levels: Li-like ions: O VI, N V, C IV**
  - With metastables, level populated by ionization from next lower charge state, plus excitation from ground
- **For low and medium-Z elements, resonance emissions primarily in the EUV/VUV**

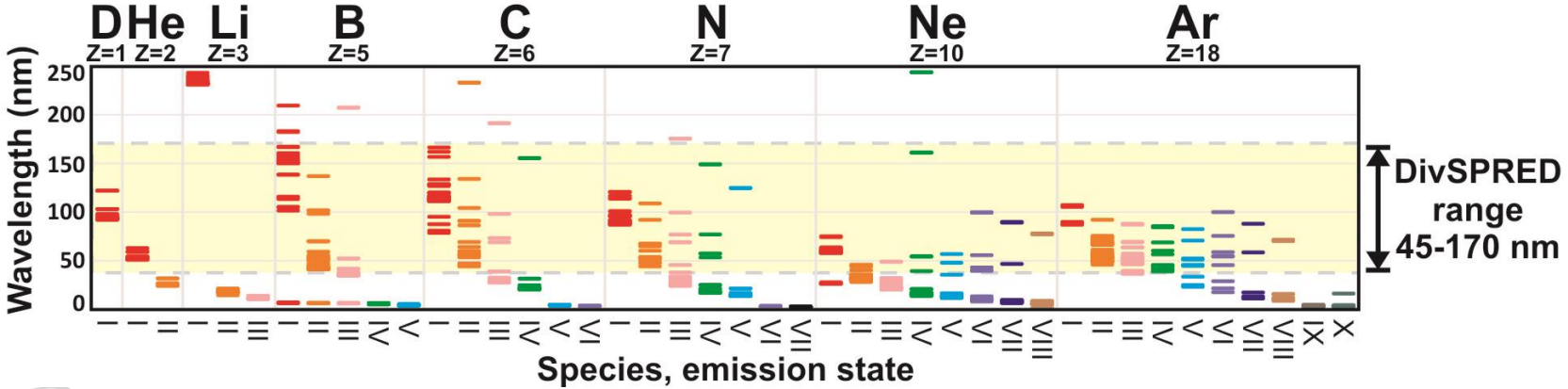

DIII-D NATIONAL FUSION FACILITY

To baseline importance of CX, UEDGE was used to find Te dependence of neutral fraction

- **UEDGE case with enhanced diffusivity chosen to match shots with best DivSPRED data**
- **Neutral fraction as a function of Te calculated in throughout grid**
  - Psi_n > 1.1 rejected to avoid main chamber recycling artifacts near X-point
  - Deuterium temperature assumed to be 3.5eV (dissociation fragments)

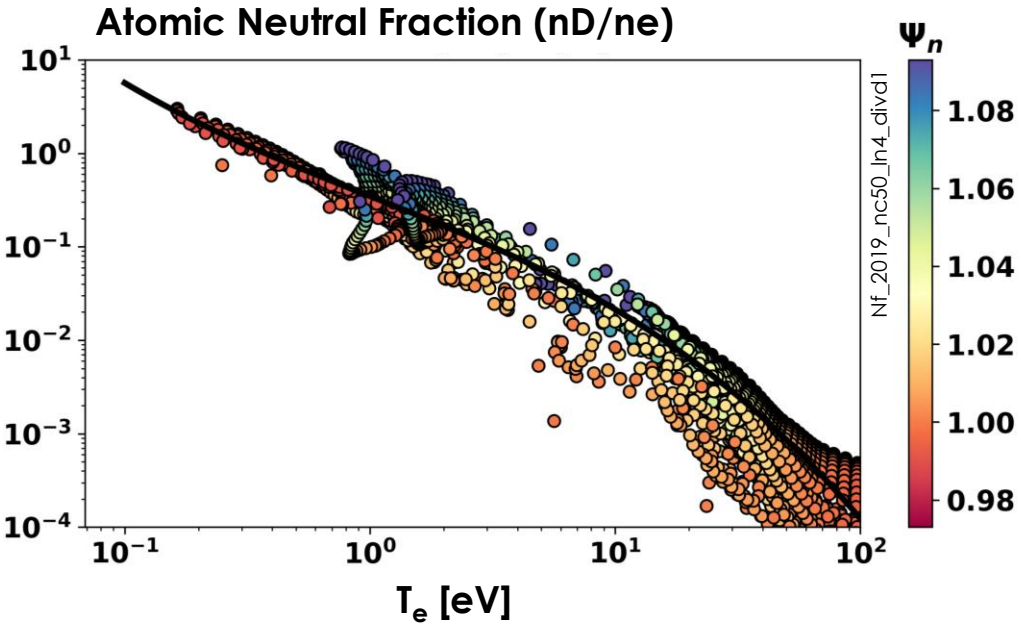

$$\frac{n_{\mathrm{D}}}{n_e} \sim \exp\left[a\log(T_e) + b(log(T_e))^3 + c\right]$$

DIII-D NATIONAL FUSION FACILITY

Including CX causes charge states to appear at higher temperatures

- Charge states C^{2+} and above have relative abundances that extend to higher temperatures
- C & C^{+} largely unaffected
- A move to more intuitively expected values (eg position of C^{2+} peak)

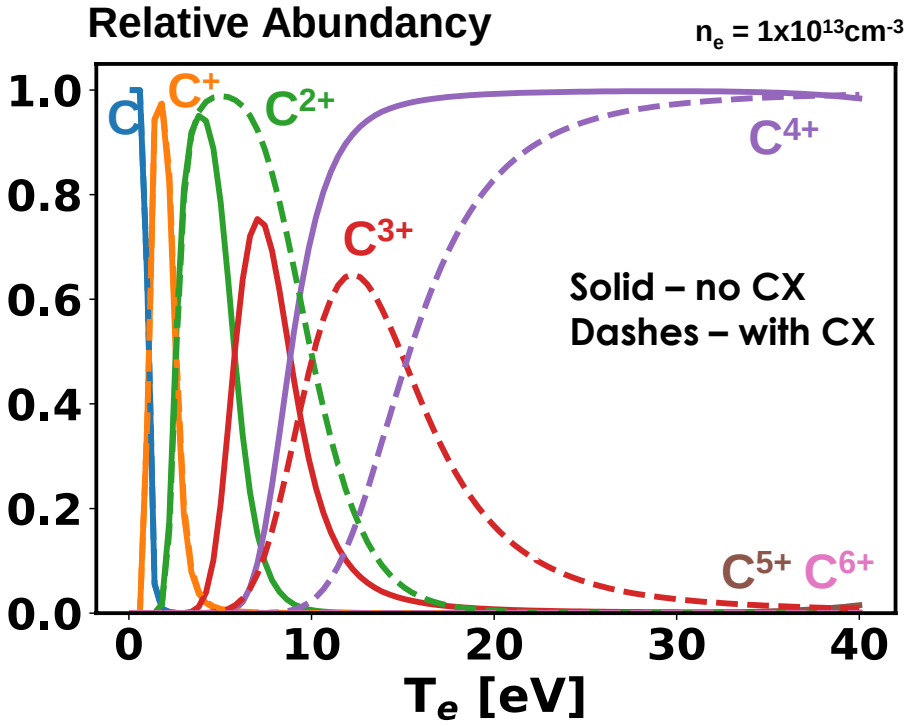

DIII-D NATIONAL FUSION FACILITY

Carbon/Nitrogen simulations comparison

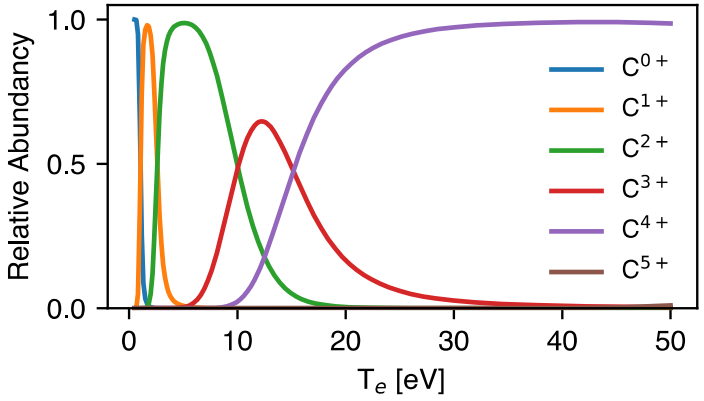

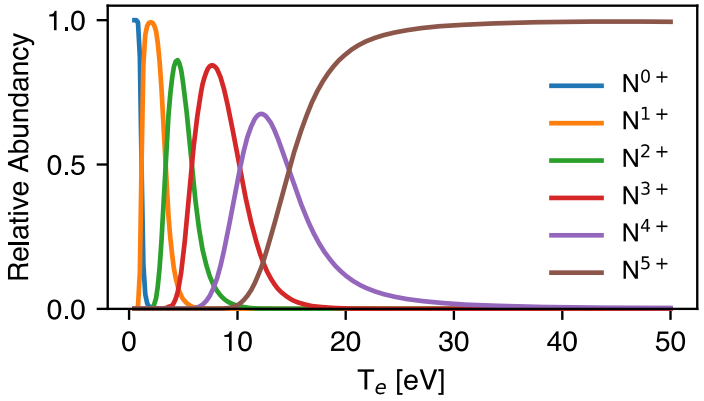

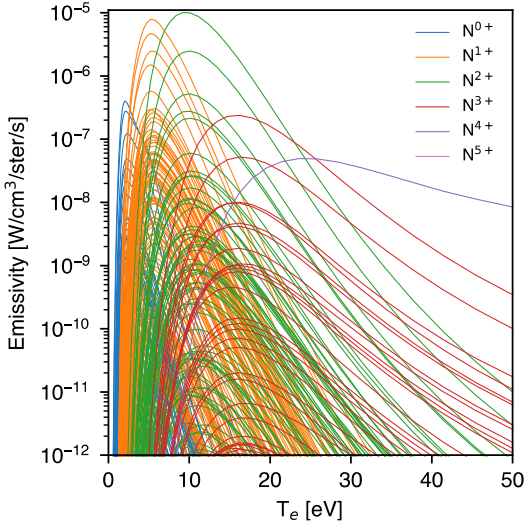

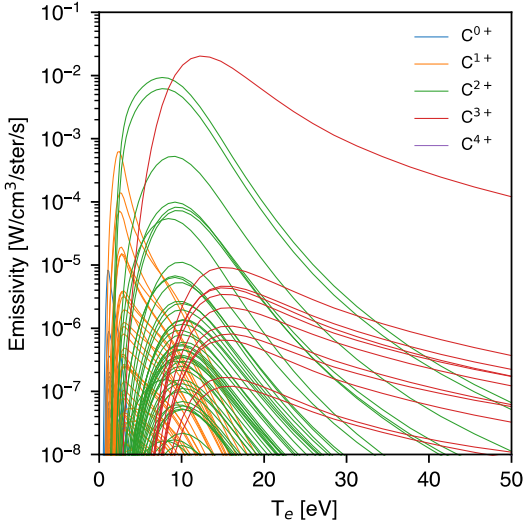

Detached nitrogen-seeded and un-seeded cases show similar impurity charge distribution in ionization front

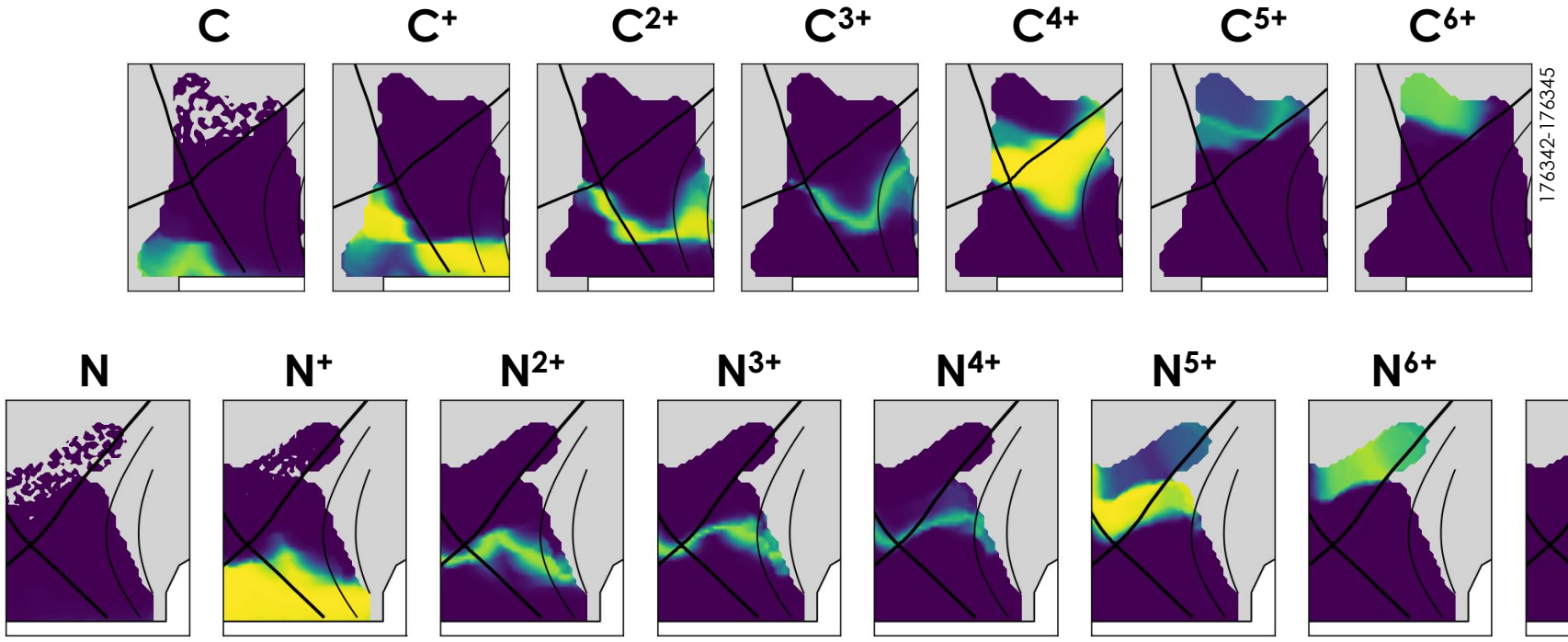

C: 2.5MW, -2T, 1.2MA, n/n_{GW}=0.8
N: 5MW, 01.8T, 0.9MA, n/n_{GW}=0.7

Fraction
0
1

DIII-D NATIONAL FUSION FACILITY

CX causes a significant broadening of ionization front in detached case, greater mixing of charge states, and reduced role of C^{4+}

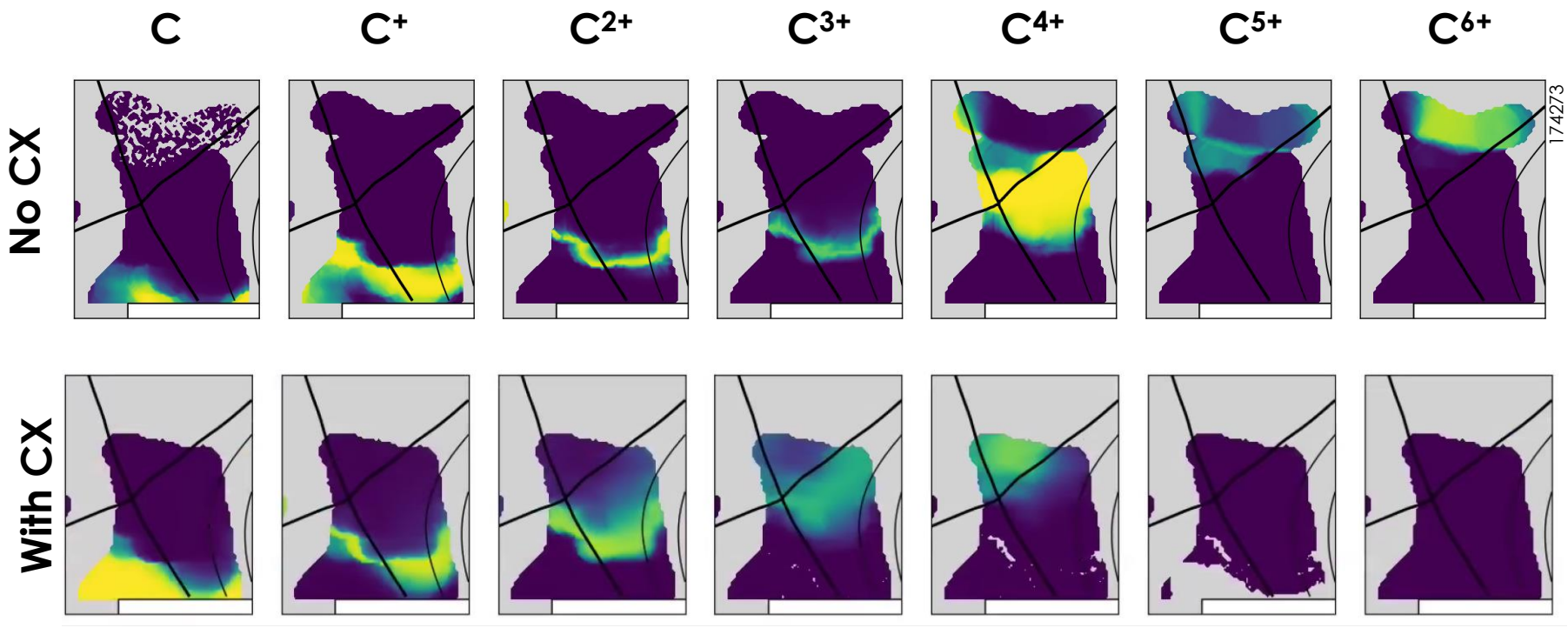

4MW, -1.8T, 0.9MA, n/n_{GW}=0.7

n_e*tau = 2E9 cm^{-3} s

NB: top DTS channel now removed also

Fraction

0 1

DIII-D NATIONAL FUSION FACILITY

Further improvement though adding transport via ne*tau

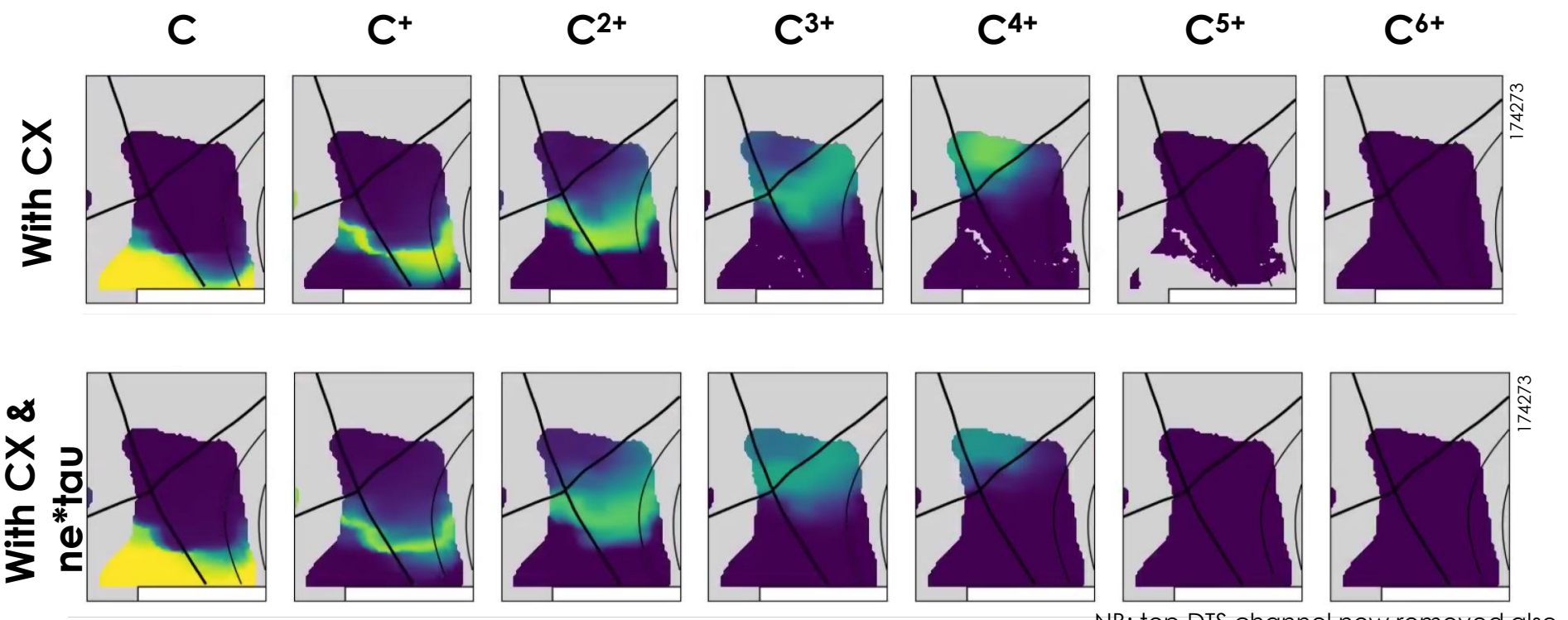

4MW, -1.8T, 0.9MA, n/n_{GW}=0.7

n_e*tau = 2E9 cm^{-3} s

NB: top DTS channel now removed also

DIII-D NATIONAL FUSION FACILITY

(Some) history of measuring impurity concentrations in fusion devices

- ***O/C/N/Mo (EUV) in Alcator: Terry, Chen, Moos, Marmar***
  - *COO-2711-3 (1977)*
- ***O/C/N/Ti (EUV) in 2XIIB mirror: Drake and Moos***
  - *NF 20 (1980) 599.*
- ***O/C/N (EUV) in TMX mirror: Allen***
  - *OCID-18883 (1981)*
- ***O/C/N/Ti (EUV) in TMX-U mirror: Yu, Allen, and Moos***
  - *JVST A 3 (1985) 1077.*
- ***Mo (VUV) in Alcator C-Mod: Graf, Terry***
  - *PhD thesis (1995)*
- ***O/C/Ni/Fe (EUV) in PBX-M and ISX-B: Isler***
  - *FED 34-35 (1997) 115.*
- ***C (EUV) in ASDEX-U: Wenzel***
  - *PPCF 41 (1999) 801.*
- ***C (VUV) in JT-60U: Nakano***
  - *NF 47 (2007) 1458, and JNM 390-391 (2009) 255.*
- ***N (visible) in ASDEX-U: Henderson***
  - *NF 58 (2018) 016047.*
- ***N (visible) in JET and ASDEX-U: Henderson***
  - *NME 18 (2019) 147.*

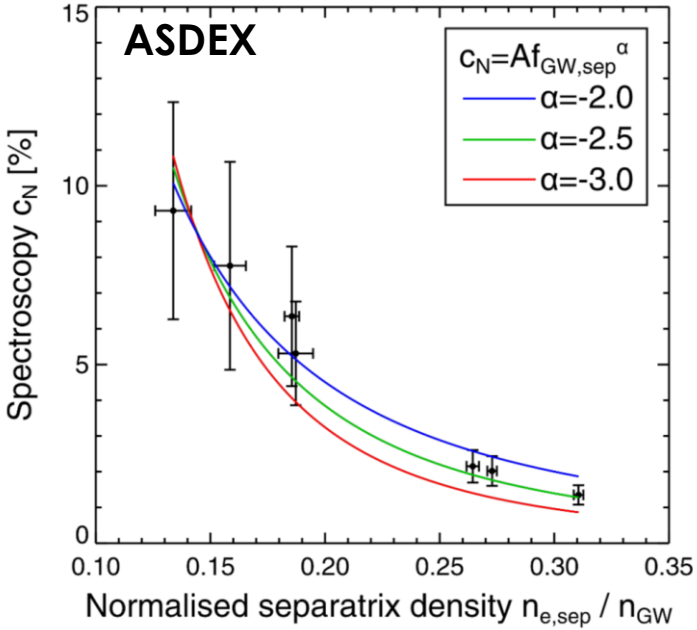

Cooling curves

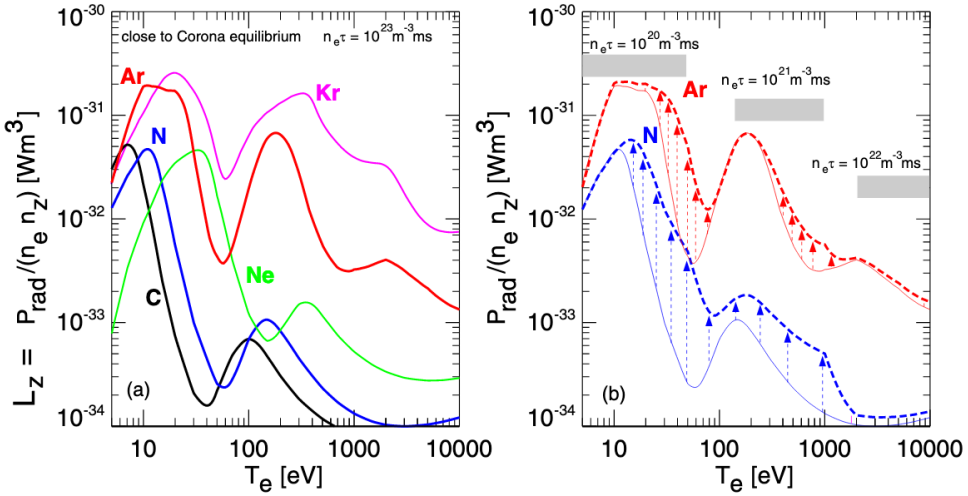

Figure 1. Radiative loss parameter L_z for seed impurities from ADAS and an electron density of 10^{20} m^{-3}, as the sum of line radiation, recombination-induced radiation and bremsstrahlung. (*a*) Data for carbon, nitrogen, neon, argon and krypton in coronal equilibrium. (*b*) Non-equilibrium enhanced values for N and Ar (dashed lines). Appropriate values for the non-equilibrium parameter $n_e\tau$ are used for the divertor and pedestal parameter regions, as indicated by the broad horizontal bars. In between the T_e values marked, a linear interpolation of $n_e\tau$ in T_e was used to obtain smooth curves.

DIII-D NATIONAL FUSION FACILITY

Kallenbach PPCF 2013

Long-pulse High Performance Plasma Relies on the Ability to Radiate the Majority of Power Injected for Plasma Heating

- **Radiated power from hot plasma includes the following processes:**
  - ***Line radiation:***
    - Deuterium, $P_{line,D0}$
    - Impurities, $P_{line,imp}$
    - Molecular radiation, P_{mol}

  } **All exist throughout the VUV/VIS/NIR**

  - ***Continuum:***
    - Bremsstrahlung (free-free emission), P_{bremss}
    - Recombining (free-bound emission), P_{recomb}
    - Blackbody radiation, $P_{blackbody}$
- **Critical to accurately measure and predict P_{rad}**

Sample spectra for each process

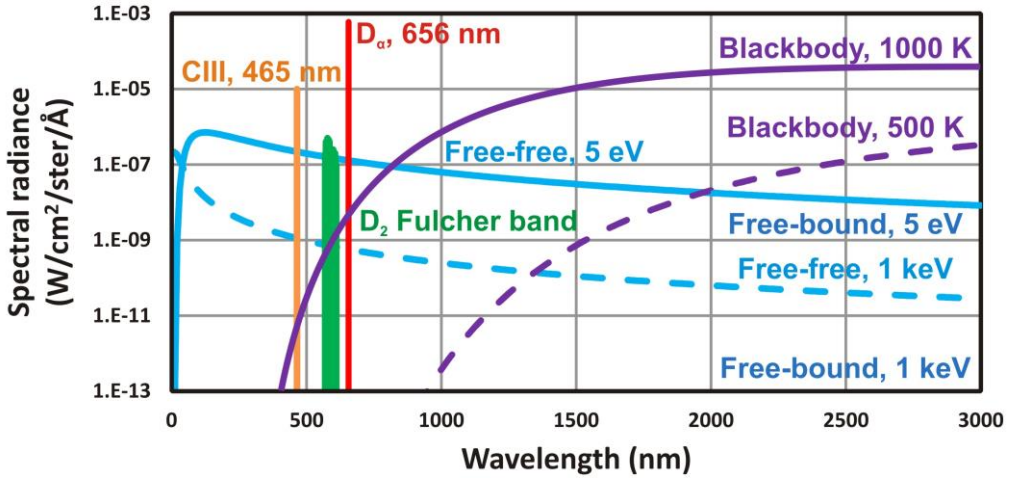

DIII-D NATIONAL FUSION FACILITY

Radiated Power in the DIII-D Divertor Includes Emissions Throughout the Visible and Infrared and EUV/VUV

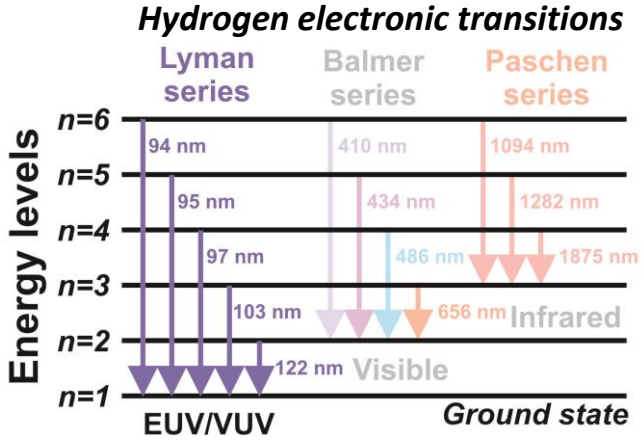

- **EUV/VUV emissions are primarily those connected to the ground state; "Resonance" lines**
  - Direct interpretation, few lines
- **Resonance lines for low-Z elements lie in EUV (10-121 nm) and/or VUV (10-200 nm)**

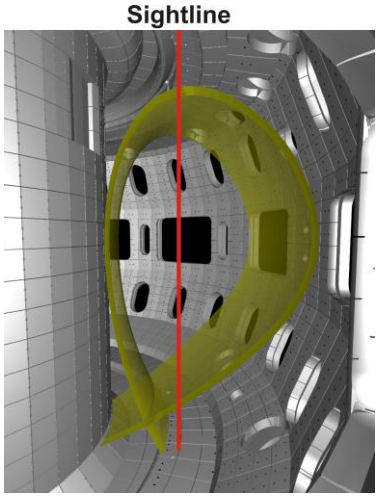

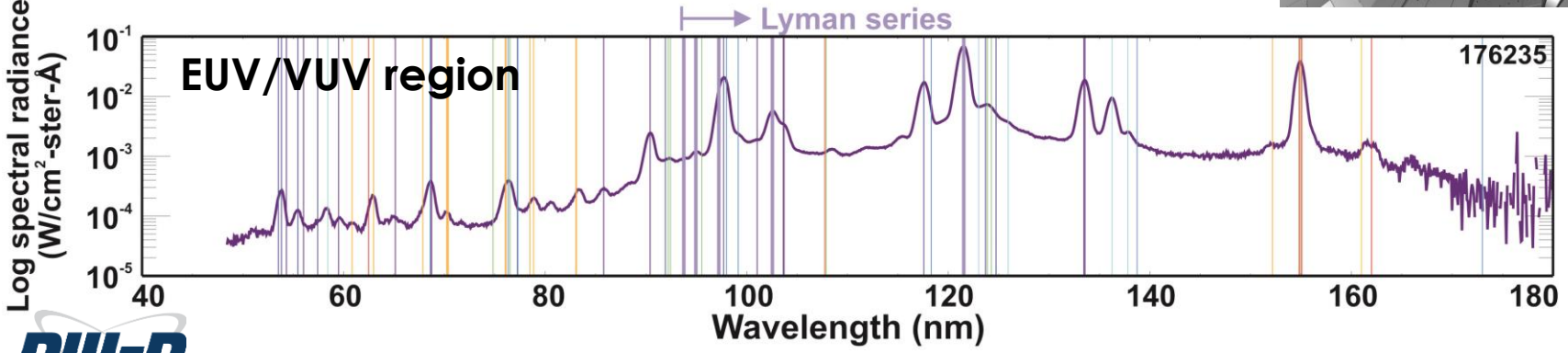

DIII-D NATIONAL FUSION FACILITY

Cross Calibration of the EUV/VUV is Made Possible Using Visible/NIR Emissions with the Same Transition Upper Level

- **Absolute sensitivity calibration is transferred from one spectral region to another**
- **Two emission lines from the same upper energy level *p***
- **Ratio of their radiances, *L*, is given by:**
- ***Independent of local conditions (T_e, n_e)***

$$\frac{L(\lambda_2)}{L(\lambda 1)} = \frac{\lambda_1}{\lambda_2}\frac{A(p \rightarrow q')}{A(p \rightarrow q)}$$

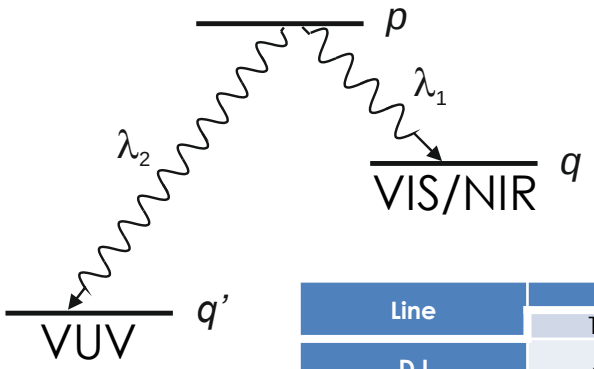

- ***Useful because NIST-calibrated light sources are available and can be directly used at UV-VIS-NIR wavelengths***

Line	EUV/VUV			VIS/NIR			$\frac{A_{Ki}EUV/VUV}{A_{Ki}VIS/NIR}$
	Transition	λ (nm)	A_{ki} (s^{-1})	Transition	λ (nm)	A_{ki} (s^{-1})	
D I	4→1 Ly-β	102.54429	5.5766E7	4→2 H_α	656.1012	4.4114E7	1.264
C II	$2s^23d\ ^2D \rightarrow 2s^22p\ ^2P^0$	68.7053	2.35E9	$2s^23d\ ^2D \rightarrow 2s^23p\ ^2P^0$	723.132	3.49E7	67.41
		68.7345	2.82E9		723.642	4.18E7	
C III	$2s3d\ ^1D \rightarrow 2s2p\ ^1P^0$	57.4281	6.24E9	$2s3d\ ^1D \rightarrow 2s3d\ ^1D$	569.592	4.27E7	146.1

DIII-D NATIONAL FUSION FACILITY

Power Accounting with Calibrated DivSPRED Agrees with Bolometry

- **Agreement through dynamic range of multiple bolometer channels**

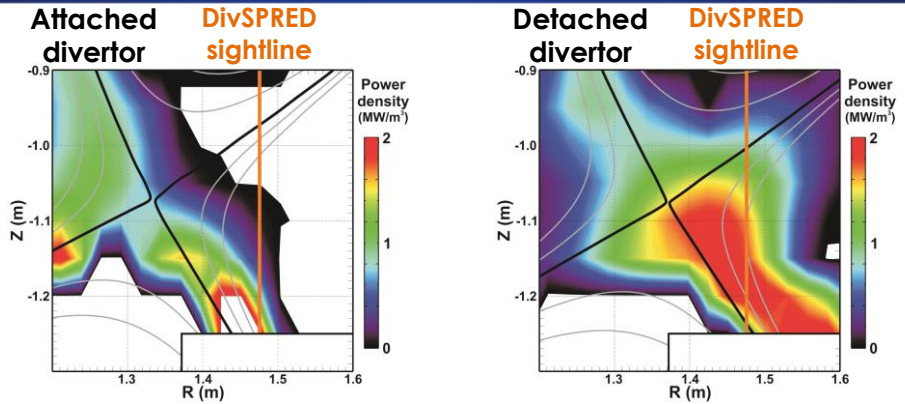

- **Validation of DivSPRED absolute intensity calibration**

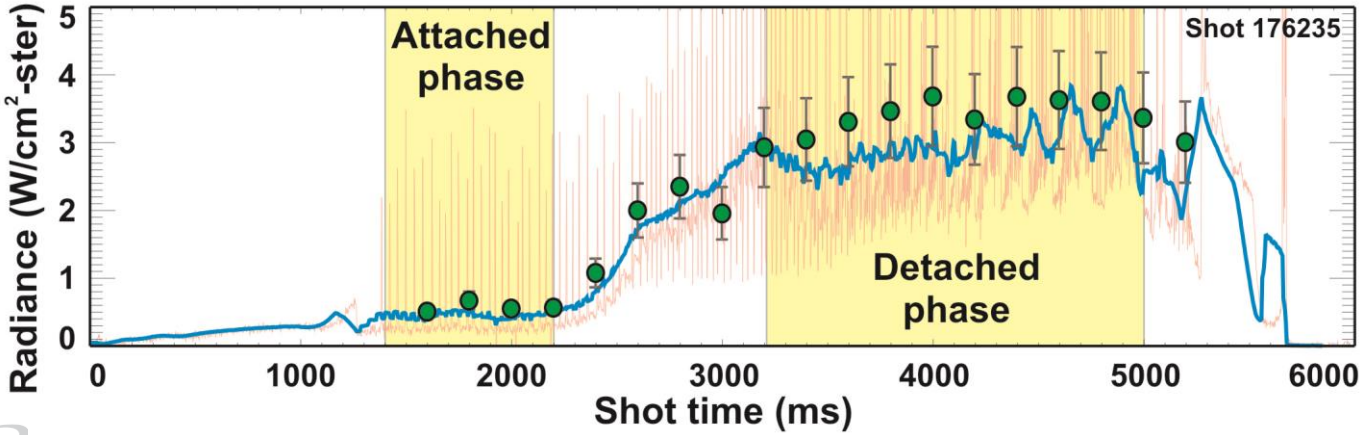

DIII-D NATIONAL FUSION FACILITY

EUV/VUV Spectrum Suggests that a Molecular Feature May be Present and Constitutes a Significant Fraction of P_{rad}

- **DivSPRED data plotted with a log Y-scale**
- **Instrumental profile characterized with an electrodeless Kr lamp**
  - Resonant lines at 116.5 and 123.6 nm
  - Primary Gaussian: FWHM ~ 0.95 nm
- **Synthetic fits to individual emission lines add up to less than the total integrated radiance in the spectra**
  - 83% of the emission spectrum is accounted for by line radiation
  - *17% is unaccounted*

DivSPRED radiance accounting, 176235
OSP view at the detachment point (n/n_{GW}=0.68)

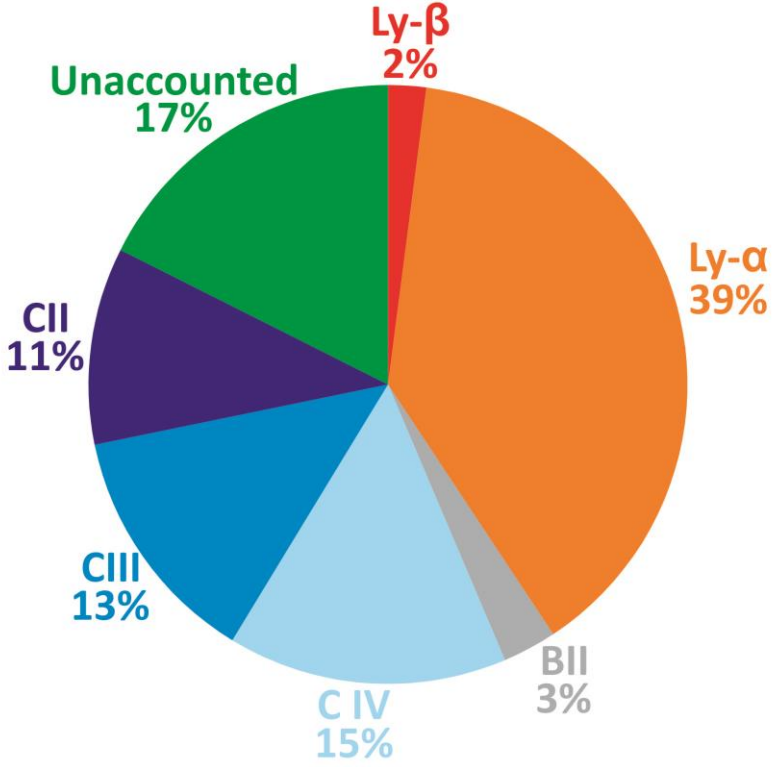

DIII-D NATIONAL FUSION FACILITY

EUV/VUV Spectrum Suggests that a Molecular Feature May be Present and Constitutes a Significant Fraction of P_{rad}

- **DivSPRED data plotted with a log Y-scale**
- **Synthetic fits to individual emission lines add up to less than the total integrated radiance in the spectra**
  - 83% of the emission spectrum is accounted for by line radiation
  - *17% is unaccounted*
- **Synthetic Lyman-Werner D_2 band**
- **Any band structure, however, is unresolvable at the DivSPRED resolution**

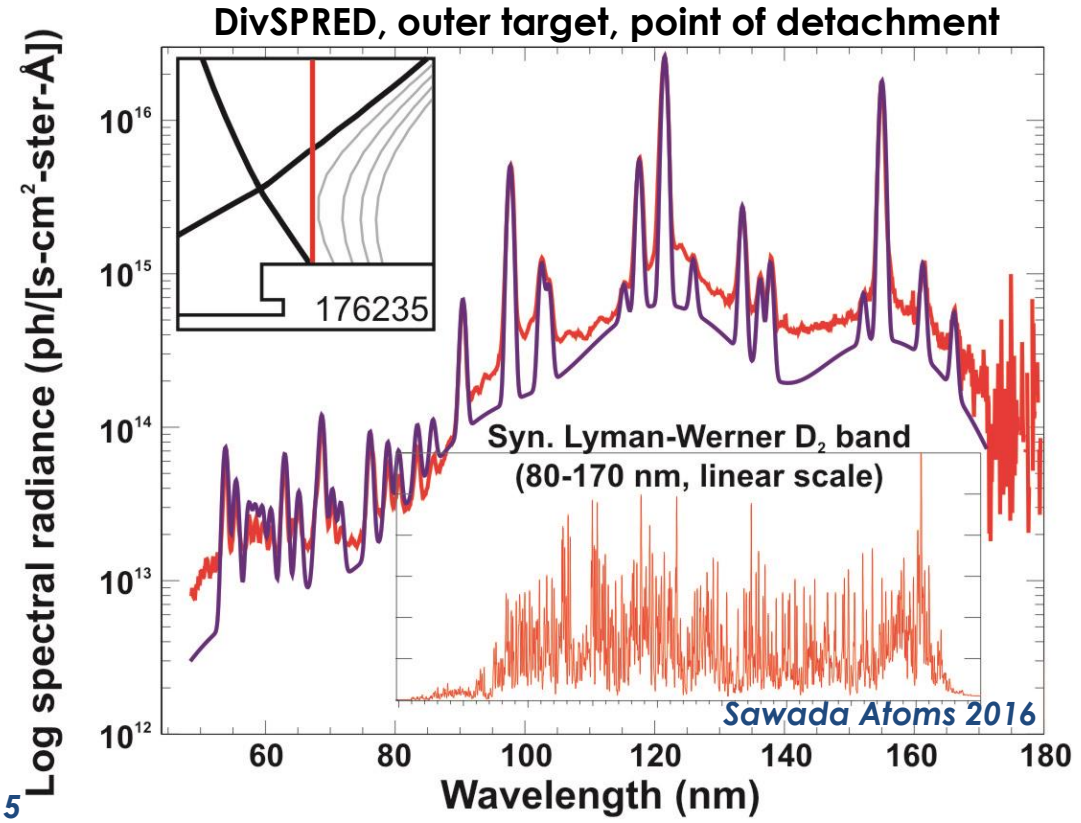

Fantz CPP 2002
Hollmann PPCF 2006
Lavrov and Umrikhin JQSRT 2015
Sawada and Goto Atoms 2016
Fantz PSST 2016

The DIII-D Divertor Diagnostic Suite Includes Necessary Tools to Quantify Divertor Emissions

- Ohmic plasmas with beam blips ($P_{ohm} \approx 0.9 – 1.4$ MW) and H-mode plasmas ($P_{ohm} + P_{inj}$ up to 13 MW), $I_P = 1.1$ MA, $B_T = 2.1$ T, both ion Bx∇B directions
- Upstream (core, SOL) density scans to achieve low-recycling, high-recycling and detached conditions
- Strike points swept across lower floor for div. profiles
- Divertor Thomson scattering (DTS) for T_e, n_e in 2D
- Vis. spectroscopy ⇒ Dα-Dγ, Fulcher band, CII, CIII
- EUV ⇒ Ly-α, Lyman-Werner bands, CIV, CIII
- Data from diagnostics are used as critical input and/or comparators to code modeling

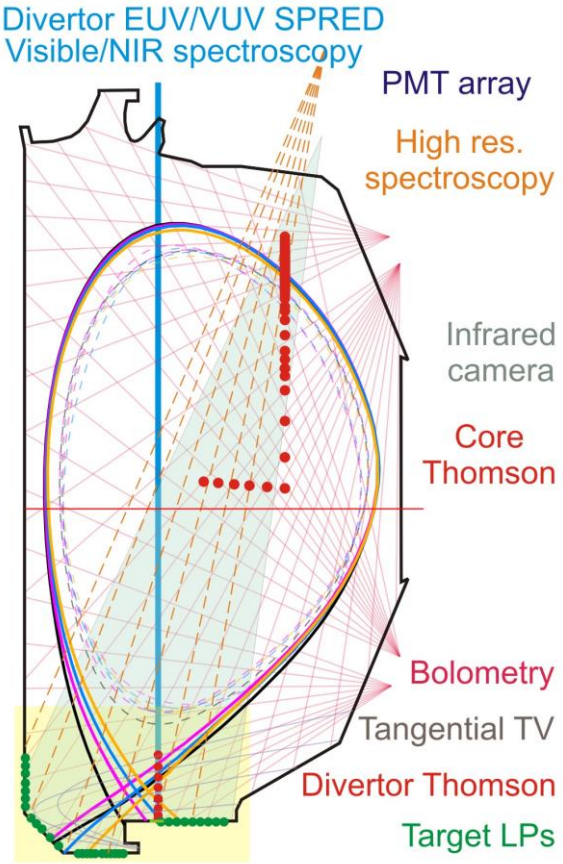

DIII-D NATIONAL FUSION FACILITY

DIII-D Diagnostic Suite Includes SXR/EUV/VUV Coverage in Both the Core (Midplane) and Divertor

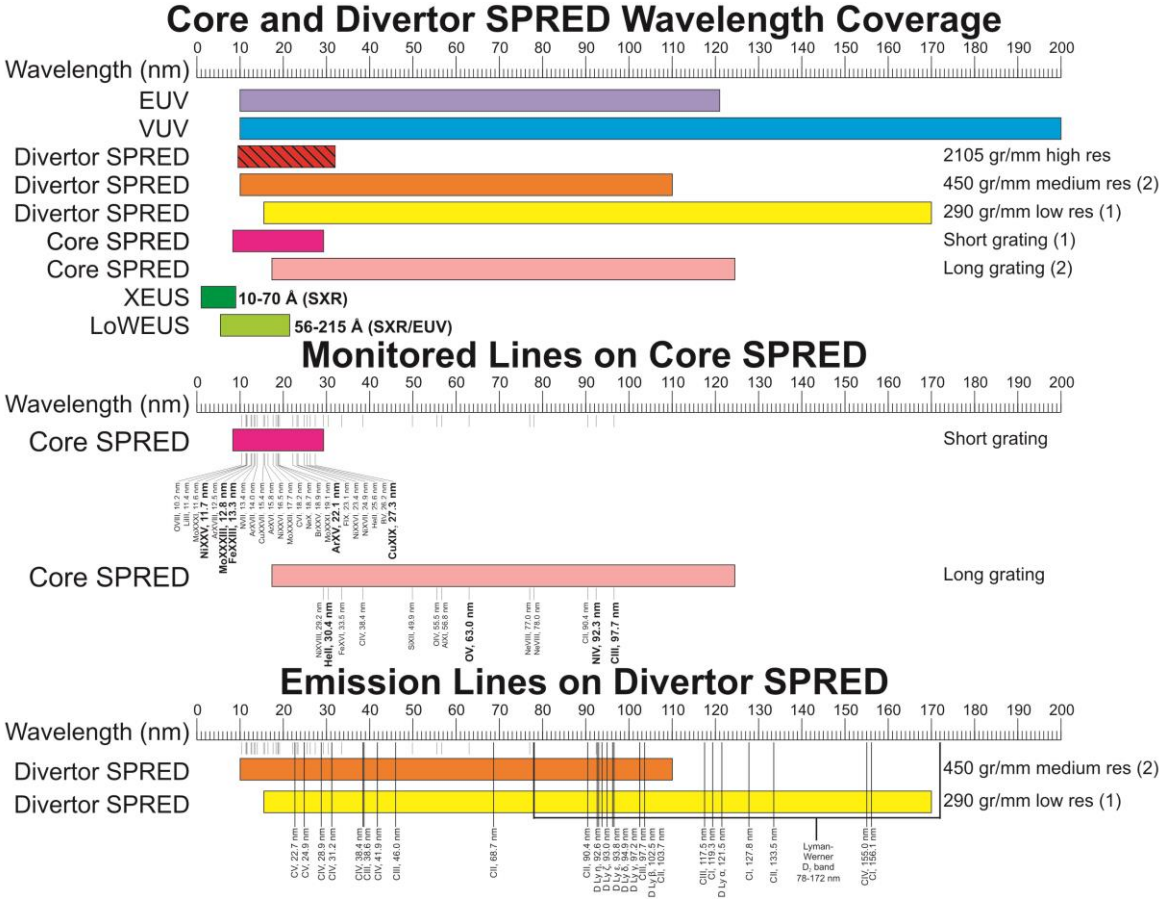

Divertor SPRED: EUV/VUV Spectroscopy Provides a Window Into the 45-170 nm Emission Region

- SPRED: Survey, Poor Resolution, Extended Domain spectrometer
- Described in R.J. Fonck, *et al.*, Applied Optics 21 (1982) 2115.
- Grazing incidence vacuum instrument designed with Schoeffel/McPherson
- Same/similar unit to that used for core SPRED on TFTR, PBX, JET, NSTX, and DIII-D
- Used on DIII-D from 1997-1999
- Absolute calibration at NIST SURF-III facility (MD)
- New CCD/sCMOS camera and optical relay, plus radiation, magnetic shielding

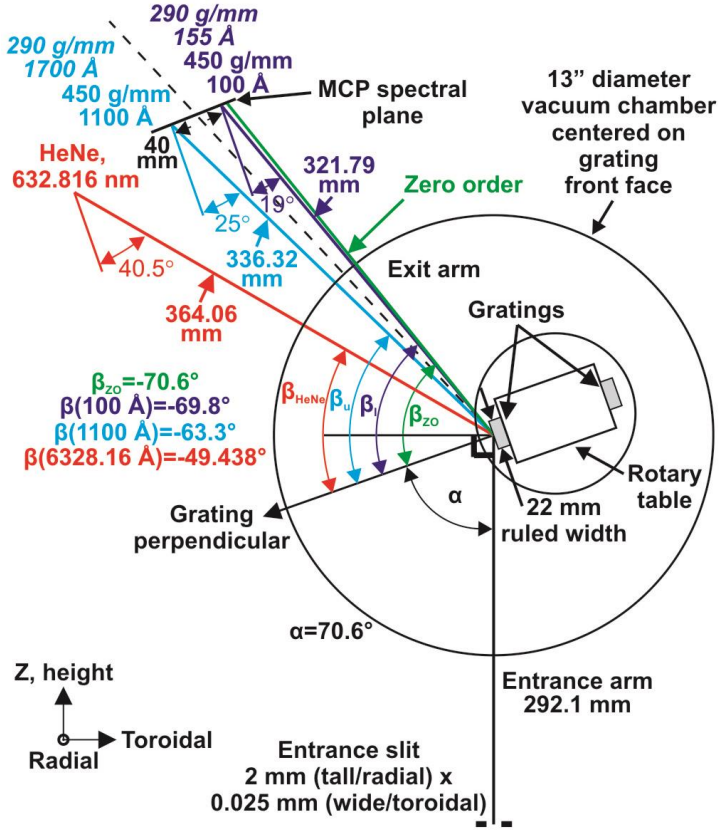

DIII-D NATIONAL FUSION FACILITY

EUV/VUV Emissions Through OSP Sweep, and Density Ramp at the OSP Suggest that Unaccounted-for Emission is Pervasive – With Wide Gaussian Instrumental

- Shot 174273: X-point sweep across lower divertor to characterize both divertor targets
- CIV dominates through most of the radial profile, except in the outer SOL
- Suggests that getting T_e, n_e profiles correct throughout the divertor region critical to matching CIV resonance emission and P_{rad}
- Shot 176235: Density ramp with DivSPRED aligned to the outer SOL
- Rapid increase in all emissions approaching detachment, then ~steady
- Unaccounted-for emission reduces approaching detachment, then also ~steady

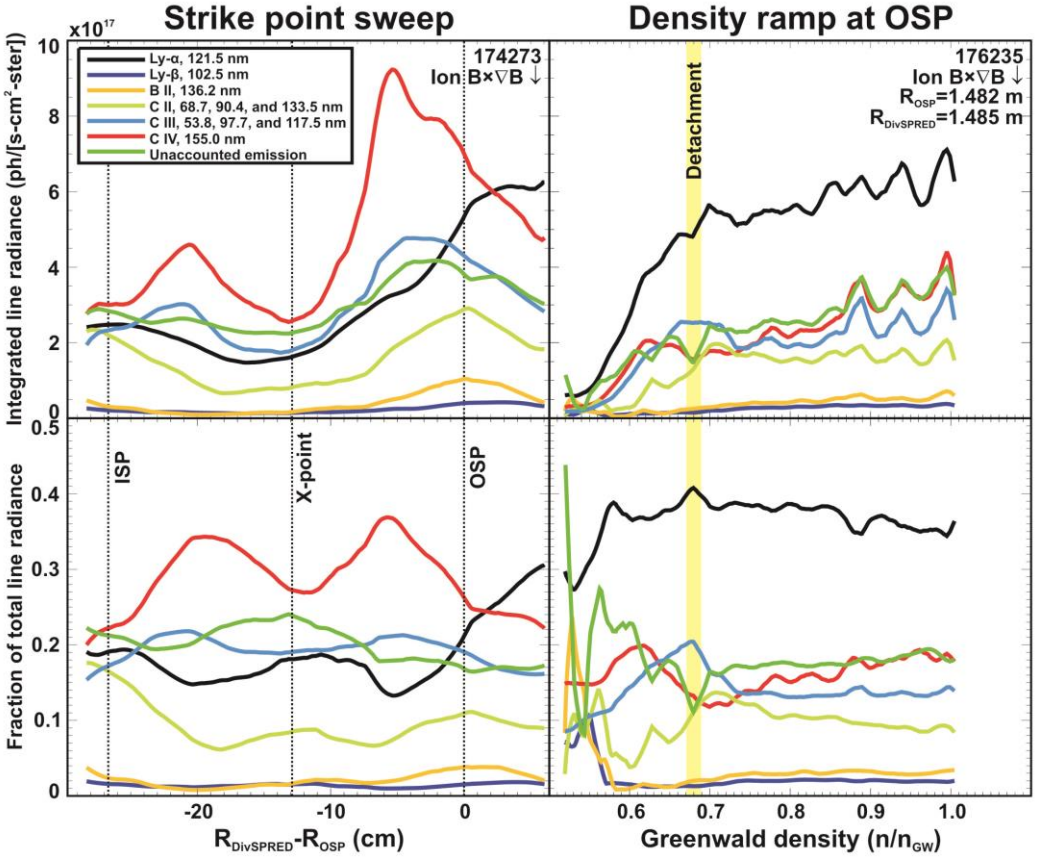

DIII-D NATIONAL FUSION FACILITY

The Solar Spectrum is Well Approximated by a Blackbody Due to Opacity in the Photosphere

- **Peak solar spectral irradiance at Earth:**
  - 2 W/m^2/nm
  - 0.16 W/m^2/ster/nm
  - 1.6x10^{-5} W/cm^2/ster/nm
  - 1.6x10^{-6} W/cm^2/ster/Å
- **Compared to divertor plasma, Ly-α line (VUV):**
  - ~0.1 W/cm^2/ster/Å
  - **63,000X brighter in the plasma**

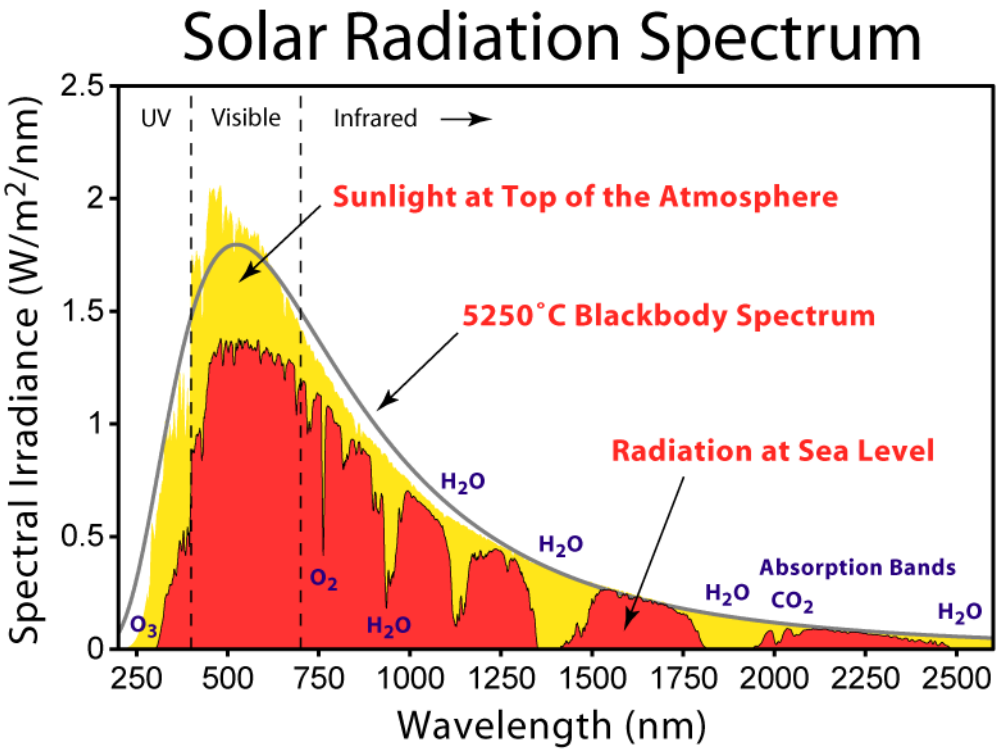

DIII-D NATIONAL FUSION FACILITY